Dynamic Setting Method of Assessment Indicators for Power Curves of Renewable Energy Sources Considering Scarcity of Reserve Resources

Minghao Cao and Jilai Yu

***Abstract*—With the increasing proportion of renewable energy sources (RESs) in power grid, the reserve resource (RR) scarcity for correcting power deviation of RESs has become a potential issue. Consequently, the power curve of RES needs to be more rigorously assessed. The RR scarcity varies during different time periods, so the values of assessment indicators should be dynamically adjusted. The assessment indicators in this paper include two aspects, i. e., deviation exemption ratio and penalty price. Firstly, this paper proposes a method for dynamically calculating the supply capacity and RR cost, primarily taking into account the operating status of thermal units, forecast information of RES, and load curve. Secondly, after clarifying the logical relationship between the degree of RR scarcity and the values of assessment indicators, this paper establishes a mapping function between them. Based on this mapping function, a dynamic setting method for assessment indicators is proposed. In the future, RES will generally be equipped with battery energy storage systems (BESSs). Reasonably utilizing BESSs to reduce the power deviation of RESs can increase the expected income of RESs. Therefore, this paper proposes a power curve optimization strategy for RESs considering self-owned BESSs. The case study demonstrates that the dynamic setting method of assessment indicators can increase the revenue of RESs while ensuring that the penalty fees paid by RESs to the grid are sufficient to cover the RR costs. Additionally, the power curve optimization strategy can help RESs further increase income and fully utilize BESSs to reduce power deviation.**

***Index Terms*—Renewable energy, battery energy storage system (BESS), power curve assessment, reserve service, parameter setting.**

NOMENCLATURE

A. Sets and Indices

D_{s1}, D_{s2}	Sets of day-ahead and intraday decision variables
n	Index of thermal units
t, Ω	Index and set of time

B. Parameters

η_{ch}, η_{dch}	Charging and discharging efficiencies of battery energy storage systems (BESSs)
δ^{T}_{up}, δ^{T}_{dn}	The maximum positive and negative climb rates of thermal units
δ^{R}_{up}, δ^{R}_{dn}	The maximum positive and negative climb rates of renewable energy source (RES)
δ_{ch}, δ_{dch}	The maximum charging and discharging rates of BESS
Δt	Scheduling period length (hour)
C^{BESS}	Construction cost of BESS (¥)
c_e, c^{T}_e	Electricity and thermal generation prices (¥/MWh)
$c^{s1}_{k,up}$, $c^{s1}_{k,dn}$	Day-ahead positive and negative reserve resource (RR) prices for segment k (¥/MWh)
$c^{s2}_{k,up}$, $c^{s2}_{k,dn}$	Intraday positive and negative RR prices for segment k (¥/MWh)
c_{st}	Start-up and shut-down prices (¥/MWh)
c_{BESS}	Unit price for using BESS (¥/MWh)
m_{max}	Setting iteration of assessment indicators
N_T	Number of thermal units
N_{day}	Number of time periods in a day
N_{s1}, N_{s2}	Segment numbers of day-ahead and intraday RR prices
P^{R}_{G}, P^{T}_{G}	Capacities of RES and thermal unit (MW)
$P^{T}_{G,n}$	Capacity of thermal unit n (MW)
P^{T}_{max}, P^{T}_{min}	The maximum and minimum power of thermal unit (MW)
P_{BESS}	Expect deviation adjustment capacity of BESS (MW)
Q_{BESS}	Capacity of BESS (MWh)
SOC_{min}	The minimum state of charge (SOC) of BESS
SOC_{max}	The maximum SOC of BESS
T_s	Cycle duration of charging and discharging (hour)

C. Variables

$\alpha^{s1}_{up,max}$	The maximum value of $\alpha^{s1}_{t,up}$

Manuscript received: February 26, 2023; revised: April 9, 2023; accepted: May 22, 2023. Date of CrossCheck: May 22, 2023. Date of online publication: July 10, 2023.

This work was supported in part by the National Natural Science Foundation of China (No. 51877049).

M. Cao (corresponding author) and J. Yu are with the Department of Electrical Engineering, Harbin Institute of Technology, Harbin, China (e-mail: caominghao_hit@foxmail.com; yupwrs@hit.edu.cn).

DOI: 10.35833/MPCE.2023.000117

$\alpha^{s1}_{dn,max}$ The maximum value of $\alpha^{s1}_{t,dn}$

$\alpha^{s1}_{t,up}$, $\alpha^{s1}_{t,dn}$, $\alpha^{s2}_{t,up}$, $\alpha^{s2}_{t,dn}$ Positive and negative power deviation exemption ratios in day-ahead and intraday stages

$\alpha^{s2}_{up,max}$ The maximum value of $\alpha^{s2}_{t,up}$

$\alpha^{s2}_{dn,max}$ The maximum value of $\alpha^{s2}_{t,dn}$

$\Delta P^{s1}_{t,up}$ Day-ahead positive power deviation of RES (MW)

$\Delta P^{s1}_{t,dn}$ Day-ahead negative power deviation of RES (MW)

$\Delta P^{s2}_{t,up}$ Intraday positive power deviation of RES (MW)

$\Delta P^{s2}_{t,dn}$ Intraday negative power deviation of RES (MW)

$\Delta P^{f1}_{t,up}$ Day-ahead positive forecast error of RES (MW)

$\Delta P^{f1}_{t,dn}$ Day-ahead negative forecast error of RES (MW)

$\Delta P^{f2}_{t,up}$ Intraday positive forecast error of RES (MW)

$\Delta P^{f2}_{t,dn}$ Intraday negative forecast error of RES (MW)

$\Delta P^{s1,f}_{t,up}$ Expectation value of $\Delta P^{s1}_{t,up}$ to optimize day-ahead curve (MW)

$\Delta P^{s1,f}_{t,dn}$ Expectation value of $\Delta P^{s1}_{t,dn}$ to optimize day-ahead curve (MW)

$\Delta P^{s2,f}_{t,up}$ Expectation value of $\Delta P^{s2}_{t,up}$ to optimize intraday curve (MW)

$\Delta P^{s2,f}_{t,dn}$ Expectation value of $\Delta P^{s2}_{t,dn}$ to optimize intraday curve (MW)

$\Delta P^{tag}_{t,up}$ Expectation charging power of BESS (MW)

$\Delta P^{tag}_{t,dn}$ Expectation discharging power of BESS (MW)

$C^{R,s1}_{t,up}$ Penalty fee for $\Delta P^{s1}_{t,up}$ (¥)

$C^{R,s1}_{t,dn}$ Penalty fee for $\Delta P^{s1}_{t,dn}$ (¥)

$C^{R,s2}_{t,up}$ Penalty fee for $\Delta P^{s2}_{t,up}$ (¥)

$C^{R,s2}_{t,dn}$ Penalty fee for $\Delta P^{s2}_{t,dn}$ (¥)

$C^{R,e}_{t}$ Income of RES from electricity charges (¥)

$C^{s1}_{t,up}$, $C^{s1}_{t,dn}$ Day-ahead positive and negative RR costs (¥)

$C^{s2}_{t,up}$, $C^{s2}_{t,dn}$ Intraday positive and negative RR costs (¥)

C^{s}_{t} RR cost (¥)

$C^{s1}_{t,n}$, $C^{s2}_{t,n}$ Day-ahead and intraday RR costs for thermal unit n (¥)

$C^{s1}_{t,up,n}$ Positive $C^{s1}_{t,n}$ (¥)

$C^{s1}_{t,dn,n}$ Negative $C^{s1}_{t,n}$ (¥)

$C^{s2}_{t,up,n}$ Positive $C^{s2}_{t,n}$ (¥)

$C^{s2}_{t,dn,n}$ Negative $C^{s2}_{t,n}$ (¥)

C^{st}_{t} Start-up and shut-down costs at time t (¥)

$C^{st}_{t,n}$ C^{st}_{t} of thermal unit n (¥)

$C^{f1}_{t,n}$, $C^{f2}_{t,n}$ Expectation value of C^{s}_{t} to set day-ahead and intraday indicators (¥)

$C^{f1,up}_{t,up,n}$ $C^{s1}_{t,up,n}$ considering positive power deviation of RES (¥)

$C^{f1,up}_{t,dn,n}$ $C^{s1}_{t,dn,n}$ considering positive power deviation of RES (¥)

$C^{f1,dn}_{t,up,n}$ $C^{s1}_{t,up,n}$ considering negative power deviation of RES (¥)

$C^{f1,dn}_{t,dn,n}$ $C^{s1}_{t,dn,n}$ considering negative power deviation of RES (¥)

$C^{f2,up}_{t,up,n}$ $C^{s2}_{t,up,n}$ considering positive power deviation of RES (¥)

$C^{f2,up}_{t,dn,n}$ $C^{s2}_{t,dn,n}$ considering positive power deviation of RES (¥)

$C^{f2,dn}_{t,up,n}$ $C^{s2}_{t,up,n}$ considering negative power deviation of RES (¥)

$C^{f2,dn}_{t,dn,n}$ $C^{s2}_{t,dn,n}$ considering negative power deviation of RES (¥)

$C^{st,f1}_{t,n}$ $C^{st}_{t,n}$ without day-ahead deviation of RES (¥)

$C^{st,f2}_{t,n}$ $C^{st}_{t,n}$ without intraday deviation of RES (¥)

$C^{st,f1,up}_{t,n}$ $C^{st}_{t,n}$ with positive day-ahead deviation of RES (¥)

$C^{st,f1,dn}_{t,n}$ $C^{st}_{t,n}$ with negative day-ahead deviation of RES (¥)

$C^{st,f2,up}_{t,n}$ $C^{st}_{t,n}$ with positive intraday deviation of RES (¥)

$C^{st,f2,dn}_{t,n}$ $C^{st}_{t,n}$ with negative intraday deviation of RES (¥)

$C^{R,s}$ Total penalty fee of RES (¥)

C^{s} Total RR cost (¥)

C^{grid} Imbalance between penalty fee and RR cost (¥)

$C^{R,s}_{t}$ Penalty fee of RES (¥)

$C^{R}_{t,in}$ Profit of RES (¥)

C^{R}_{in} Total profit of RES (¥)

C^{BESS}_{t} Cost of using BESS (¥)

$C^{R,s1}_{t,in}$ Expectation value of $C^{R}_{t,in}$ to optimize day-ahead curve (¥)

$C^{R,s2}_{t,in}$ Expectation value of $C^{R}_{t,in}$ to optimize intraday curve (¥)

$C^{T}_{t,n}$ Generation cost of thermal unit n (¥)

$c^{R,s1}_{t,up}$, $c^{R,s1}_{t,dn}$ Day-ahead positive and negative penalty prices (¥/MWh)

$c^{R,s2}_{t,up}$, $c^{R,s2}_{t,dn}$ Intraday positive and negative penalty prices (¥/MWh)

$c^{R,s1}_{up,max}$ The maximum value of $c^{R,s1}_{t,up}$ (¥/MWh)

$c^{R,s1}_{up,min}$ The minimum value of $c^{R,s1}_{t,up}$ (¥/MWh)

$c^{R,s2}_{up,max}$ The maximum value of $c^{R,s2}_{t,up}$ (¥/MWh)

$c^{R,s2}_{up,min}$ The minimum value of $c^{R,s2}_{t,up}$ (¥/MWh)

$c^{R,s1}_{dn,max}$ The maximum value of $c^{R,s1}_{t,dn}$ (¥/MWh)

$c^{R,s1}_{dn,min}$ The minimum value of $c^{R,s1}_{t,dn}$ (¥/MWh)

$c^{R,s2}_{dn,max}$ The maximum value of $c^{R,s2}_{t,dn}$ (¥/MWh)

$c^{R,s2}_{dn,min}$ The minimum value of $c^{R,s2}_{t,dn}$ (¥/MWh)

$f^{c1}_{up}(\cdot)$, $f^{c1}_{dn}(\cdot)$, $f^{c2}_{up}(\cdot)$, $f^{c2}_{dn}(\cdot)$ Positive and negative RR prices in day-ahead and intraday stages

$f^{s1}(\cdot)$, $f^{s2}(\cdot)$ Probability density distributions of r^{f1}_{t} and r^{f2}_{t}

P^{R}_{t} Actual power curve of RES (MW)

P^{s1}_{t}, P^{s2}_{t} Day-ahead and intraday power curves of RES (MW)

$P^{s1}_{t,max}$ The maximum value of P^{s1}_{t} without day-ahead penalty (MW)

$P^{s1}_{t,min}$ The minimum value of P^{s1}_{t} without day-ahead

	penalty (MW)
$P^{s2}_{t,\max}$	The maximum value of P^{s2}_t without intraday penalty (MW)
$P^{s2}_{t,\min}$	The minimum value of P^{s2}_t without intraday penalty (MW)
P^{f1}_t, P^{f2}_t	Day-ahead and intraday forecast power of RES (MW)
$P^{R,f1}_t$	Day-ahead forecast power of P^R_t (MW)
$P^{R,f2}_t$	Intraday forecast power of P^R_t (MW)
P^T_t	Actual power of thermal unit at time t (MW)
$P^T_{t,\max}$	The maximum power of thermal unit at time t (MW)
$P^T_{t,\min}$	The minimum power of thermal unit at time t (MW)
$P^{T,s1}_t$	Day-ahead curve of thermal unit (MW)
$P^{T,s2}_t$	Intraday curve of thermal unit (MW)
$P^{T,s1}_{t,n}$	$P^{T,s1}_t$ of thermal unit n (MW)
$P^{T,s2}_{t,n}$	$P^{T,s2}_t$ of thermal unit n (MW)
$P^{T,f1}_{t,n}$	$P^{T,s1}_{t,n}$ without deviation of RES (MW)
$P^{T,f2}_{t,n}$	$P^{T,s2}_{t,n}$ without deviation of RES (MW)
$P^{T,f1,up}_{t,n}$	$P^{T,s1}_{t,n}$ considering positive deviation of RES (MW)
$P^{T,f1,dn}_{t,n}$	$P^{T,s1}_{t,n}$ considering negative deviation of RES (MW)
$P^{T,f2,up}_{t,n}$	$P^{T,s2}_{t,n}$ considering positive deviation of RES (MW)
$P^{T,f2,dn}_{t,n}$	$P^{T,s2}_{t,n}$ considering negative deviation of RES (MW)
P^L_t	Load curve at time t (MW)
P^{ch}_t, P^{dch}_t	Charging and discharging power of BESS (MW)
$P^{ch,f}_t$	Forecast value of P^{ch}_t to optimize intraday curve (MW)
$P^{dch,f}_t$	Forecast value of P^{dch}_t to optimize intraday curve (MW)
$P^{BESS}_{t,up,s1}$	Day-ahead positive adjustment ability of BESS (MW)
$P^{BESS}_{t,dn,s1}$	Day-ahead negative adjustment ability of BESS (MW)
$P^{BESS}_{t,up,s2}$	Intraday positive adjustment ability of BESS (MW)
$P^{BESS}_{t,dn,s2}$	Intraday negative adjustment ability of BESS (MW)
r^{f1}_t, r^{f2}_t	Day-ahead and intraday forecast error ratios of RES
SOC_t	SOC of BESS
SOC^f_t	Expectation SOC of BESS
u_t	Operating status of thermal unit
$\Delta u^{f1}_{t,n}$, $\Delta u^{f2}_{t,n}$	Start-close action of thermal unit n without day-ahead and intraday power deviations of RES
$\Delta u^{f1,up}_{t,n}$, $\Delta u^{f1,dn}_{t,n}$, $\Delta u^{f2,up}_{t,n}$, $\Delta u^{f2,dn}_{t,n}$	Start-close action of thermal unit n considering positive and negative power deviations of RES in day-ahead and intraday stages

D. Abbreviations and Symbols

ch, dch	Charging and discharging actions of BESS
f1, f2	Day-ahead and intraday forecast or expectation values
s1, s2, R	Day-ahead, intraday, and actual generation stages

I. Introduction

THE proportion of renewable energy sources (RESs) in power system is increasing [1] and RES will become one of the main power sources [2]. Due to the strong randomness and volatility of the output of RESs as well as the forecast accuracy of power [3], [4], it is necessary for power grid to provide extra reserve resources (RRs) to correct the power deviations of RESs. The distribution of RR demand for RESs is uneven at different time, and the ability and cost of power grid to provide RR also vary with time, which may result in an RR scarcity during some periods [5]. RR in power grid is mainly provided by hydro and thermal units, but hydro units have seasonal differences and the development of thermal units is restricted by environmental regulations [6]. At the same time, the rapid growth of RES generation leads to an increase in RR demand, resulting in an imbalance between RR supply and demand. There is an urgent need to discuss how to assess the accuracy of RES power curves more rigorously, in order to control the RR demand from the source and improve the utilization efficiency of RR in the power grid [7].

In recent years, there have been studies on how to reduce the pressure of grid reserve by improving the accuracy of RES power curve execution. Reference [8] proposed a short-term economic dispatch model, which considers that the power forecast accuracy of RES will change over time. By setting different accuracy requirements at different time scales, the model fits the natural distribution of power forecast accuracy for RES [9]. Reference [10] proposed a power curve optimization strategy for RES composed of wind and solar energy. In this strategy, the self-owned BESS is used to dynamically limit [11] the power ramp rate and correct the deviation of the short-term power curve. Reference [12] established a model for evaluating the power forecast deviation of wind and solar energy and designed a stochastic planning model that considered line transmission capacity, uncertainty of RES output, energy storage, and gas-fired units which have flexible peak-shaving capabilities. Reference [13] proposed an optimal scheduling strategy for incorporating the remaining reserve resources into the intraday ancillary service market by predicting the power adjustment margin of wind energy. The above-mentioned studies mainly discussed how to reduce the power fluctuations and forecast deviations of RESs, and analyzed the effect of improving the accuracy of RES power curves in helping power grid maintain stable operation [14]-[16]. In existing references, the insufficient RRs in power grid are often supplemented through bidding in the ancillary service market. References [17] and [18] proposed a form of auxiliary service market organization based on joint operation entities, and discussed the scheduling plan assignment method, pricing, and settlement

process under this situation. Reference [19] analyzed the opportunity cost in the ancillary service market and applied it to user systems such as intelligent heating, ventilation, and air conditioning [20], [21]. Reference [22] designed a hybrid energy storage system consisting of BESS and supercapacitors for providing RR. In addition, an energy management method was also proposed to improve the operating efficiency of system. Equipped with small- and medium-sized BESS [23]-[25], RES can enhance its power deviation control ability, which is an important measure to ensure the high-quality development of RESs. Optimizing the power curve of RES considering self-owned BESS can significantly reduce power deviation and the RR demand [26]-[28].

The existing research can be mainly categorized into two aspects, i.e., methods for reducing power fluctuations and deviations of RESs, and approaches to exploring the RR supply. However, there are few studies that focus on the dynamic assessment of power curve deviation to address the RR scarcity caused by RESs. In addition, the assessment indicators in existing studies often rely on market clearing results, which cannot effectively guide RESs in optimizing power curves. It will increase the difficulty in optimizing RES power curves and reduce the using efficiency of RRs in the power grid.

This paper proposes a calculation method for the degree of RR scarcity and designs a dynamic setting method of assessment indicators based on it. As shown in Fig. 1, RES needs to determine power curves for power grid in day-ahead and intraday stages before actually transmitting power to the grid.

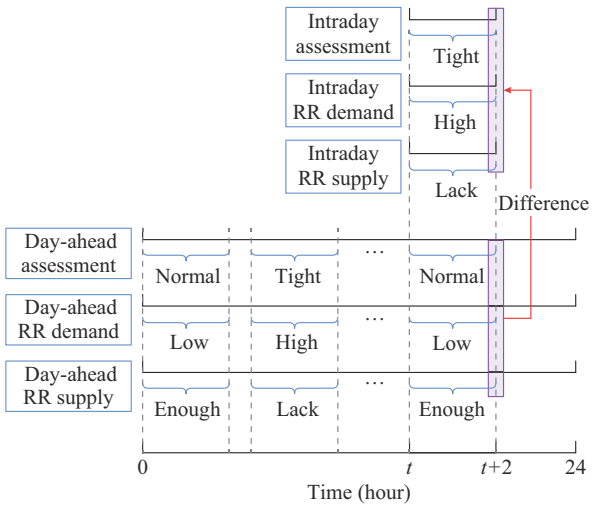

Fig. 1. Dynamic setting process of assessment indicators.

Detailedly, RES needs to determine the power curve for the next 24 hours in day-ahead stage and adjust it in intraday stage. The prediction accuracy of RESs improves as the time scale is shortened, so this rolling power curve correction model can fit the power forecast characteristics of RESs. The ability and cost of the power grid to provide RR depend on the operating states of each unit and vary during different periods. Meanwhile, the expected RR demand from RESs also varies during different periods. These two factors contribute to the dynamic changes of RR scarcity. To address the above situation, the power grid should dynamically adjust the assessment indicators based on the degree of RR scarcity. When RR is scarce, the power grid should tighten deviation exemption ratio or increase the penalty prices. When RR is abundant, the power grid should adopt basic assessment indicators to reduce the pressure of RES power curve tracking. Based on this concept, this paper estimates the RR demand of RES according to the power forecast information of RES, and estimates the RR supply capacity and price based on the load rate of thermal power units. Based on this, this paper establishes a quantitative relationship between RR supply capacity, RR price, and assessment indicators values, and designs a power curve optimization strategy of RES considering self-owned BESS.

The main contributions of this paper are summarized as follows.

1) This paper establishes a quantitative relationship among RR supply capacity/price, RR demand, the operating status of thermal units, power forecast information of RES, and assessment indicator values. In addition, based on the degree of RR scarcity, the assessment indicators are dynamically adjusted to effectively transfer the RR supply pressure from the grid side to the RES side, so that RES can optimize the power curve more reasonably and accurately and respond to the reserve demand of grid in real time.

2) The penalty fees paid by RES to the power grid can cover the RR costs paid by the grid to thermal units, implementing the RR cost sharing principle of “who uses, who pays”. This approach takes into account the interests of both RES and the grid, making the assessment scheme more easily promotable.

3) The power curve optimization strategy of RES proposed in this paper considers the deviation correction effect of self-owned BESS at both the day-ahead and intraday time scales, which can improve the accuracy of RES power curve and increase the profit of RES.

II. Setting Strategy and Rationality Evaluation of Assessment Indicators

This section quantifies the degree of RR scarcity and dynamically adjusts the assessment indicators accordingly. In addition, an evaluation index for the reasonableness of assessment indicators is established, which mainly includes two aspects: whether the penalty fees can cover the RR costs and whether the profit of RES can be maintained at a reasonable level.

A. Model for Assessment Indicators

RES needs to optimize the power curve for the next day in 15-min intervals during [0, 24]hours, and then adjusts the power curve again 2 hours before the actual transmission to the grid. Assessment indicators include two components: deviation exemption ratios ($\alpha^{s1}_{t,up}$, $\alpha^{s1}_{t,dn}$, $\alpha^{s2}_{t,up}$, and $\alpha^{s2}_{t,dn}$) and penalty prices ($c^{R,s1}_{t,up}$, $c^{R,s1}_{t,dn}$, $c^{R,s2}_{t,up}$, and $c^{R,s2}_{t,dn}$). According to the deviation exemption ratio and power curve, the range exempt from penalties, i.e., $[P^{s1}_{t,min}, P^{s1}_{t,max}]$ and $[P^{s2}_{t,min}, P^{s2}_{t,max}]$, can be calculated. Only the power beyond this range will be penalized, and the penalty price is used to calculate the penalty fees based on the amount of penalized power.

The model for the assessment indicators is as follows.

$$\begin{cases} P_{t,\max}^{\mathrm{s1}} = (1+\alpha_{t,\mathrm{up}}^{\mathrm{s1}})P_t^{\mathrm{s1}} \\ P_{t,\min}^{\mathrm{s1}} = (1-\alpha_{t,\mathrm{dn}}^{\mathrm{s1}})P_t^{\mathrm{s1}} \end{cases} \tag{1}$$

$$\begin{cases} \Delta P_{t,\mathrm{up}}^{\mathrm{s1}} = P_t^{\mathrm{s2}} - P_{t,\max}^{\mathrm{s1}} & \forall P_t^{\mathrm{s2}} \ge P_{t,\max}^{\mathrm{s1}} \\ \Delta P_{t,\mathrm{dn}}^{\mathrm{s1}} = P_{t,\min}^{\mathrm{s1}} - P_t^{\mathrm{s2}} & \forall P_t^{\mathrm{s2}} < P_{t,\min}^{\mathrm{s1}} \end{cases} \tag{2}$$

$$\begin{cases} C_{t,\mathrm{up}}^{\mathrm{R,s1}} = c_{t,\mathrm{up}}^{\mathrm{R,s1}} \Delta P_{t,\mathrm{up}}^{\mathrm{s1}} \Delta t \\ C_{t,\mathrm{dn}}^{\mathrm{R,s1}} = c_{t,\mathrm{dn}}^{\mathrm{R,s1}} \Delta P_{t,\mathrm{dn}}^{\mathrm{s1}} \Delta t \end{cases} \tag{3}$$

$$\begin{cases} P_{t,\max}^{\mathrm{s2}} = (1+\alpha_{t,\mathrm{up}}^{\mathrm{s2}})P_t^{\mathrm{s2}} \\ P_{t,\min}^{\mathrm{s2}} = (1-\alpha_{t,\mathrm{dn}}^{\mathrm{s2}})P_t^{\mathrm{s2}} \end{cases} \tag{4}$$

$$\begin{cases} \Delta P_{t,\mathrm{up}}^{\mathrm{s2}} = P_t^{\mathrm{R}} - P_{t,\max}^{\mathrm{s2}} & \forall P_t^{\mathrm{R}} \ge P_{t,\max}^{\mathrm{s2}} \\ \Delta P_{t,\mathrm{dn}}^{\mathrm{s2}} = P_{t,\min}^{\mathrm{s2}} - P_t^{\mathrm{R}} & \forall P_t^{\mathrm{R}} < P_{t,\min}^{\mathrm{s2}} \end{cases} \tag{5}$$

$$\begin{cases} C_{t,\mathrm{up}}^{\mathrm{R,s2}} = c_{t,\mathrm{up}}^{\mathrm{R,s2}} \Delta P_{t,\mathrm{up}}^{\mathrm{s2}} \Delta t \\ C_{t,\mathrm{dn}}^{\mathrm{R,s2}} = c_{t,\mathrm{dn}}^{\mathrm{R,s2}} \Delta P_{t,\mathrm{dn}}^{\mathrm{s2}} \Delta t \end{cases} \tag{6}$$

Additionally, the electricity income of RES is only settled for the part that does not exceed $P_{t,\max}^{\mathrm{s2}}$. Otherwise, the grid needs to increase the positive deviation assessment price, which would create a confusing price difference.

$$C_t^{\mathrm{R,e}} = \begin{cases} c_{\mathrm{e}} P_{t,\max}^{\mathrm{s2}} \Delta t & \forall P_t^{\mathrm{R}} \ge P_{t,\max}^{\mathrm{s2}} \\ c_{\mathrm{e}} P_t^{\mathrm{R}} \Delta t & \forall P_t^{\mathrm{R}} < P_{t,\max}^{\mathrm{s2}} \end{cases} \tag{7}$$

The day-ahead and intraday assessment indicators are dynamically adjusted based on the current RR scarcity. The grid will set the day-ahead assessment indicators for the next 24 hours before RES optimizes the day-ahead power curve, and set the intraday assessment indicators before RES adjusts the power curve, in order to timely guide RES.

B. Process of Setting Assessment Indicators

Before introducing the method for setting assessment indicators, it is necessary to first establish a model for the operation constraints of thermal units and the calculation method of RR costs.

The operation constraints of thermal units mainly include two parts: ① the positive and negative power change rates should be kept within the limited range; and ② the thermal units need to be shut down when the power is below the minimum technical output. The model of the operation constraints is expressed as follows.

$$u_t = \{0, 1\} \tag{8}$$

$$u_t = \begin{cases} 1 & P_{\min}^{\mathrm{T}} \le P_t^{\mathrm{T}} \le P_{\max}^{\mathrm{T}}, \forall t \\ 0 & P_t^{\mathrm{T}} = 0, \forall t \end{cases} \tag{9}$$

$$\begin{cases} (P_t^{\mathrm{T}} - P_{t-1}^{\mathrm{T}})/\Delta t \le \delta_{\mathrm{up}}^{\mathrm{T}} P_{\mathrm{G}}^{\mathrm{T}} & \forall t \\ (P_{t-1}^{\mathrm{T}} - P_t^{\mathrm{T}})/\Delta t \le \delta_{\mathrm{dn}}^{\mathrm{T}} P_{\mathrm{G}}^{\mathrm{T}} & \forall t \end{cases} \tag{10}$$

Thermal units need to declare the RR prices in segments. When the RR is actually called by the grid, the grid settles the RR prices of each unit based on their load rates and clears them from low to high. In addition, the RR costs should also include start-up and shut-down costs. The calculation model is given as:

$$\begin{cases} f_{\mathrm{up}}^{\mathrm{c1}}(P) = c_{k,\mathrm{up}}^{\mathrm{s1}} & \forall P \in \left[\dfrac{P_{\mathrm{G}}^{\mathrm{T}}}{N_{\mathrm{s1}}}(k-1), \dfrac{P_{\mathrm{G}}^{\mathrm{T}}}{N_{\mathrm{s1}}} k \right] \\ f_{\mathrm{dn}}^{\mathrm{c1}}(P) = c_{k,\mathrm{dn}}^{\mathrm{s1}} & \forall P \in \left[\dfrac{P_{\mathrm{G}}^{\mathrm{T}}}{N_{\mathrm{s1}}}(k-1), \dfrac{P_{\mathrm{G}}^{\mathrm{T}}}{N_{\mathrm{s1}}} k \right] \end{cases} \tag{11}$$

$$\begin{cases} C_{t,\mathrm{up}}^{\mathrm{s1}} = \Delta t \displaystyle\int_{P_t^{\mathrm{T,s1}}}^{P_t^{\mathrm{T,s2}}} f_{\mathrm{up}}^{\mathrm{c1}}(P)\,\mathrm{d}P & \forall P_t^{\mathrm{T,s2}} \ge P_t^{\mathrm{T,s1}} \\ C_{t,\mathrm{dn}}^{\mathrm{s1}} = \Delta t \displaystyle\int_{P_t^{\mathrm{T,s2}}}^{P_t^{\mathrm{T,s1}}} f_{\mathrm{dn}}^{\mathrm{c1}}(P)\,\mathrm{d}P & \forall P_t^{\mathrm{T,s2}} < P_t^{\mathrm{T,s1}} \end{cases} \tag{12}$$

$$\begin{cases} f_{\mathrm{up}}^{\mathrm{c2}}(P) = c_{k,\mathrm{up}}^{\mathrm{s2}} & \forall P \in \left[\dfrac{P_{\mathrm{G}}^{\mathrm{T}}}{N_{\mathrm{s2}}}(k-1), \dfrac{P_{\mathrm{G}}^{\mathrm{T}}}{N_{\mathrm{s2}}} k \right] \\ f_{\mathrm{dn}}^{\mathrm{c2}}(P) = c_{k,\mathrm{dn}}^{\mathrm{s2}} & \forall P \in \left[\dfrac{P_{\mathrm{G}}^{\mathrm{T}}}{N_{\mathrm{s2}}}(k-1), \dfrac{P_{\mathrm{G}}^{\mathrm{T}}}{N_{\mathrm{s2}}} k \right] \end{cases} \tag{13}$$

$$\begin{cases} C_{t,\mathrm{up}}^{\mathrm{s2}} = \Delta t \displaystyle\int_{P_t^{\mathrm{T,s2}}}^{P_t^{\mathrm{T}}} f_{\mathrm{up}}^{\mathrm{c2}}(P)\,\mathrm{d}P & \forall P_t^{\mathrm{T}} \ge P_t^{\mathrm{T,s2}} \\ C_{t,\mathrm{dn}}^{\mathrm{s2}} = \Delta t \displaystyle\int_{P_t^{\mathrm{T}}}^{P_t^{\mathrm{T,s2}}} f_{\mathrm{dn}}^{\mathrm{c2}}(P)\,\mathrm{d}P & \forall P_t^{\mathrm{T}} < P_t^{\mathrm{T,s2}} \end{cases} \tag{14}$$

$$C_t^{\mathrm{s}} = C_{t,\mathrm{up}}^{\mathrm{s1}} + C_{t,\mathrm{dn}}^{\mathrm{s1}} + C_{t,\mathrm{up}}^{\mathrm{s2}} + C_{t,\mathrm{dn}}^{\mathrm{s2}} \quad \forall \left| u_t - u_{t+1} \right| = 0 \tag{15}$$

$$C_t^{\mathrm{s}} = C_t^{\mathrm{st}} = c_{\mathrm{st}} P_{\mathrm{G}}^{\mathrm{T}} \quad \forall \left| u_t - u_{t+1} \right| = 1 \tag{16}$$

Here is an example to help introduce the calculation method of RR costs. Assuming that the RR prices of thermal unit are divided into 10 segments, as shown in Table I, other parameters of thermal units are set as: $c_{\mathrm{st}} = 1000$ ¥/MW, $P_{\mathrm{G}}^{\mathrm{T}} = 500$ MW, $P_{\max}^{\mathrm{T}} = 500$ MW, $P_{\min}^{\mathrm{T}} = 150$ MW, $\delta_{\mathrm{up}}^{\mathrm{T}} = \delta_{\mathrm{dn}}^{\mathrm{T}} = 0.3$ (the maximum load change rate of the thermal unit is 2%/min). The day-ahead, intraday, and actual power curves of the thermal units are shown in Fig. 2, and the RR costs during each period are shown in Fig. 3.

TABLE I
RR SEGMENTED PRICING OF THERMAL UNITS

k	$c_{k,\mathrm{up}}^{\mathrm{s1}}$ (¥/MWh)	$c_{k,\mathrm{dn}}^{\mathrm{s1}}$ (¥/MWh)	$c_{k,\mathrm{up}}^{\mathrm{s2}}$ (¥/MWh)	$c_{k,\mathrm{dn}}^{\mathrm{s2}}$ (¥/MWh)
1				
2				
3				
4	0	800	0	1200
5	0	600	0	900
6	0	400	0	600
7	0	0	0	0
8	400	0	600	0
9	600	0	900	0
10	800	0	1200	0

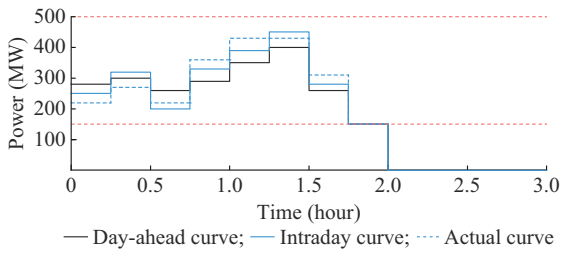

Fig. 2. Day-ahead, intraday, and actual power curves of thermal units.

As shown in Fig. 2 and Fig. 3, the RR cost is divided into three parts, i. e., the day-ahead RR cost, the intraday RR cost, and the start-up/shut-down cost of thermal units.

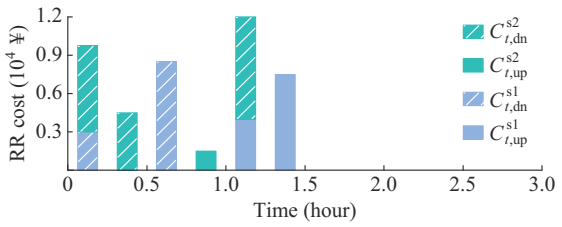

Fig. 3. RR costs during each period.

When calculating the day-ahead RR cost, the first step is to calculate the adjustment amount of the intraday power curve of thermal unit compared with the day-ahead power curve, and the second step is to calculate the RR price based on the load rate of thermal unit at that time and the RR segmented pricing information. The process for calculating intraday RR cost is similar to day-ahead RR cost, only the load rate of thermal unit and RR segmented pricing information are different.

The start-up/shut-down cost is high and occurs less frequent. If the power curve of the thermal unit already includes a start-up/shut-down plan, this part of start-up/shut-down cost should not be paid by RES. The start-up/shut-down cost of the thermal unit at hour 2 in Fig. 2 belongs to this case. Only when the thermal unit is forced to start up/shut down due to a significant power deviation caused by RES and the original plan does not include start-up/shut-down plan, will the start-up/shut-down cost be included in the penalty fees paid by RES.

The values of the day-ahead and intraday assessment indicators during each period need to be dynamically adjusted based on the operational status of the thermal units.

1) Process of Setting Day-ahead Assessment Indicators

Before optimizing the day-ahead power curve of thermal unit, RES needs to submit a forecast curve for the next 24 hours to the power grid. The power grid predicts the load rate of each thermal unit based on the forecasts and then predicts the supply capacity and RR price. After that, the power grid can set the day-ahead assessment indicators accordingly. The flowchart for the above process is shown in Fig. 4.

According to the process shown in Fig. 4, *Step 1* is to calculate the expected day-ahead power deviation of RES during each period based on the forecast curve and the probability density function of the forecast deviation ratio of RES.

$$r_t^{\mathrm{fl}} = (P - P_t^{\mathrm{fl}})/P_t^{\mathrm{fl}} \tag{17}$$

$$\begin{cases} \Delta P_{t,\mathrm{up}}^{\mathrm{fl}} = \displaystyle\int_{P_t^{\mathrm{fl}}}^{P_{\mathrm{G}}^{\mathrm{R}}} f^{\mathrm{s1}}(r_t^{\mathrm{fl}})(P - P_t^{\mathrm{fl}})\mathrm{d}P \\ \Delta P_{t,\mathrm{dn}}^{\mathrm{fl}} = \displaystyle\int_{0}^{P_t^{\mathrm{fl}}} f^{\mathrm{s1}}(r_t^{\mathrm{fl}})(P_t^{\mathrm{fl}} - P)\mathrm{d}P \end{cases} \tag{18}$$

Steps 2 and *3* in Fig. 4 are performed simultaneously. The day-ahead power curve of the thermal unit can be estimated based on the day-ahead power forecast of RES and the technical parameters of the thermal unit. By combining the expected day-ahead power deviation of RES and the RR segmented pricing of thermal unit, the RR costs during each period can be estimated.

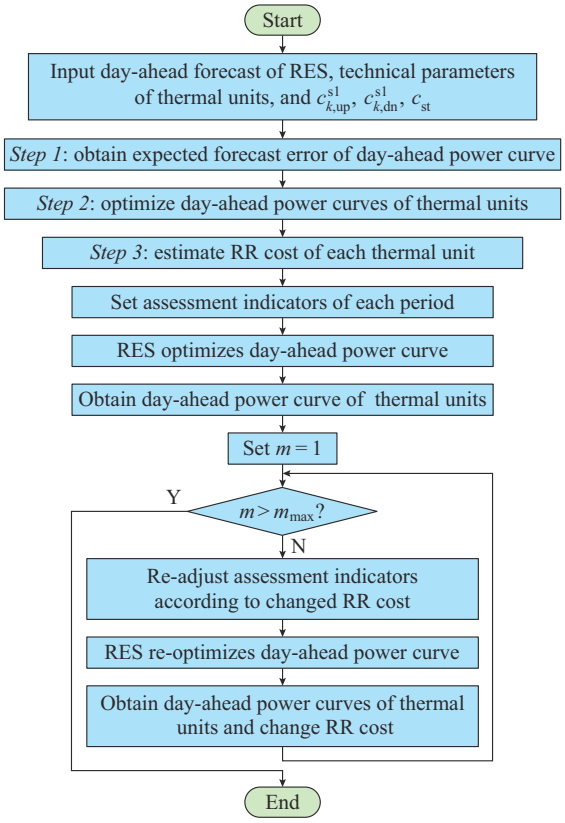

Fig. 4. Process for setting the day-ahead assessment indicators.

Estimating RR costs for each time period is done in two steps.

1) Calculate the output of the thermal unit without considering the forecast deviation of RES, i.e., $P_{t,n}^{\mathrm{T,fl}}$, and then calculate the output of thermal unit considering positive and negative day-ahead forecast deviations of RES, i.e., $P_{t,n}^{\mathrm{T,fl,up}}$ and $P_{t,n}^{\mathrm{T,fl,dn}}$, respectively.

2) Calculate the RR costs during each period based on the adjustment amount of $P_{t,n}^{\mathrm{T,fl,up}}$ and $P_{t,n}^{\mathrm{T,fl,dn}}$ compared with $P_{t,n}^{\mathrm{T,fl}}$ as well as the expected load rate of the thermal unit.

The optimization objective aims to minimize the RR costs and generation cost, as shown in (19). Additionally, constraints $P_{t,n}^{\mathrm{T,fl}}$, $P_{t,n}^{\mathrm{T,fl,up}}$ and $P_{t,n}^{\mathrm{T,fl,dn}}$ are subject to (8)-(10).

$$\min \sum_{n=1}^{N_{\mathrm{T}}} C_{t,n}^{\mathrm{fl}}(D_{\mathrm{s1}}) \tag{19}$$

$$C_{t,n}^{\mathrm{fl}} = C_{t,\mathrm{up},n}^{\mathrm{fl,up}} + C_{t,\mathrm{dn},n}^{\mathrm{fl,up}} + C_{t,\mathrm{up},n}^{\mathrm{fl,dn}} + C_{t,\mathrm{dn},n}^{\mathrm{fl,dn}} - C_{t,n}^{\mathrm{st,fl}} + C_{t,n}^{\mathrm{st,fl,up}} + C_{t,n}^{\mathrm{st,fl,dn}} + C_{t,n}^{\mathrm{T}} \tag{20}$$

$$C_{t,n}^{\mathrm{T}} = c_{\mathrm{e}}^{\mathrm{T}} P_{t,n}^{\mathrm{T,fl}} \Delta t \tag{21}$$

$$P_t^{\mathrm{L}} = P_t^{\mathrm{fl}} + \sum_{n=1}^{N_{\mathrm{T}}} P_{t,n}^{\mathrm{T,fl}} \quad \forall t \tag{22}$$

$$P_t^{\mathrm{L}} = P_t^{\mathrm{fl}} + \Delta P_{t,\mathrm{up}}^{\mathrm{fl}} + \sum_{n=1}^{N_{\mathrm{T}}} P_{t,n}^{\mathrm{T,fl,up}} \quad \forall t \tag{23}$$

$$P_t^{\mathrm{L}} = P_t^{\mathrm{fl}} - \Delta P_{t,\mathrm{dn}}^{\mathrm{fl}} + \sum_{n=1}^{N_{\mathrm{T}}} P_{t,n}^{\mathrm{T,fl,dn}} \quad \forall t \tag{24}$$

$$\begin{cases} C_{t,\mathrm{up},n}^{\mathrm{fl,up}} = \Delta t \displaystyle\int_{P_{t,n}^{\mathrm{T,fl}}}^{P_{t,n}^{\mathrm{T,fl,up}}} f_{\mathrm{up}}^{\mathrm{c1}}(P)\,\mathrm{d}P \quad \forall P_{t,n}^{\mathrm{T,fl,up}} \geq P_{t,n}^{\mathrm{T,fl}} \\ C_{t,\mathrm{dn},n}^{\mathrm{fl,up}} = \Delta t \displaystyle\int_{P_{t,n}^{\mathrm{T,fl,up}}}^{P_{t,n}^{\mathrm{T,fl}}} f_{\mathrm{dn}}^{\mathrm{c1}}(P)\,\mathrm{d}P \quad \forall P_{t,n}^{\mathrm{T,fl,up}} < P_{t,n}^{\mathrm{T,fl}} \end{cases} \tag{25}$$

$$\begin{cases} C_{t,\mathrm{up},n}^{\mathrm{fl,dn}} = \Delta t \displaystyle\int_{P_{t,n}^{\mathrm{T,fl}}}^{P_{t,n}^{\mathrm{T,fl,dn}}} f_{\mathrm{up}}^{\mathrm{c1}}(P)\,\mathrm{d}P \quad \forall P_{t,n}^{\mathrm{T,fl,dn}} \geq P_{t,n}^{\mathrm{T,fl}} \\ C_{t,\mathrm{dn},n}^{\mathrm{fl,dn}} = \Delta t \displaystyle\int_{P_{t,n}^{\mathrm{T,fl,dn}}}^{P_{t,n}^{\mathrm{T,fl}}} f_{\mathrm{dn}}^{\mathrm{c1}}(P)\,\mathrm{d}P \quad \forall P_{t,n}^{\mathrm{T,fl,dn}} < P_{t,n}^{\mathrm{T,fl}} \end{cases} \tag{26}$$

$$\begin{cases} C_{t,n}^{\mathrm{st,fl}} = c_{\mathrm{st}} P_{\mathrm{G},n}^{\mathrm{T}} \Delta u_{t,n}^{\mathrm{fl}} \\ C_{t,n}^{\mathrm{st,fl,up}} = c_{\mathrm{st}} P_{\mathrm{G},n}^{\mathrm{T}} \Delta u_{t,n}^{\mathrm{fl,up}} \\ C_{t,n}^{\mathrm{st,fl,dn}} = c_{\mathrm{st}} P_{\mathrm{G},n}^{\mathrm{T}} \Delta u_{t,n}^{\mathrm{fl,dn}} \end{cases} \tag{27}$$

Based on the RR costs and forecast power curve of RES, the deviation exemption ratios ($\alpha_{t,\mathrm{up}}^{\mathrm{s1}}$, $\alpha_{t,\mathrm{dn}}^{\mathrm{s1}}$) and penalty prices ($c_{t,\mathrm{up}}^{\mathrm{R,s1}}$, $c_{t,\mathrm{dn}}^{\mathrm{R,s1}}$) can be calculated for each period. If the RR is relatively abundant and the power deviation of some RESs will not increase the RR cost, the values of the deviation exemption ratios are set to be the base values. The greater the amount of RR that can be provided for free, the larger the values of $\alpha_{t,\mathrm{up}}^{\mathrm{s1}}$ and $\alpha_{t,\mathrm{dn}}^{\mathrm{s1}}$ are. If the free RR during a certain time period is not sufficient to adjust the expected RES power deviation, the penalty prices $c_{t,\mathrm{up}}^{\mathrm{R,s1}}$ and $c_{t,\mathrm{dn}}^{\mathrm{R,s1}}$ are set based on the RR cost during that period. The higher the RR cost, the larger the values of $c_{t,\mathrm{up}}^{\mathrm{R,s1}}$ and $c_{t,\mathrm{dn}}^{\mathrm{R,s1}}$.

The purpose of setting a basic value for the assessment indicators is to prevent the indicators from being excessively relaxed, ensuring that it remains above the basic level and satisfies the constraints shown in (28) and (29).

$$\begin{cases} \alpha_{t,\mathrm{up}}^{\mathrm{s1}} \in [0, \alpha_{\mathrm{up,max}}^{\mathrm{s1}}] \quad \forall t \\ \alpha_{t,\mathrm{dn}}^{\mathrm{s1}} \in [0, \alpha_{\mathrm{dn,max}}^{\mathrm{s1}}] \quad \forall t \end{cases} \tag{28}$$

$$\begin{cases} c_{t,\mathrm{up}}^{\mathrm{R,s1}} \in [c_{\mathrm{up,min}}^{\mathrm{R,s1}}, c_{\mathrm{up,max}}^{\mathrm{R,s1}}] \quad \forall t \\ c_{t,\mathrm{dn}}^{\mathrm{R,s1}} \in [c_{\mathrm{dn,min}}^{\mathrm{R,s1}}, c_{\mathrm{dn,max}}^{\mathrm{R,s1}}] \quad \forall t \end{cases} \tag{29}$$

Otherwise, during some RR-abundant periods, the assessment indicators may be excessively loose, which will incorrectly guide RES to adopt more aggressive power curve optimization strategies, contradicting the original intention of improving the tracking ability of RES power curve. In addition, the RR costs during periods of unplanned reserve caused by the unplanned start-up and shut-down and stop of thermal units will be significantly higher than those during other periods. If an upper limit is not set for $c_{t,\mathrm{up}}^{\mathrm{R,s1}}$, RES will bear huge operational pressure during such periods. In some scenarios, the unplanned start-up and shut-down of thermal units are an inevitable result of RR insufficiency in the power grid, indicating that the grid may not be able to absorb so much RES. Therefore, this part of the cost should not be entirely borne by RES. In fact, the RR costs and penalty fees during other periods are also not entirely balanced. The proposed method for setting the assessment indicators aims to achieve dynamic balance between RR costs and penalty fees in long-term operation. Therefore, the assessment indicators should have upper limits.

The set of base values of assessment indicators is shown in (30). The calculation method of deviation exemption ratios is shown in (31).

$$D_{\mathrm{s1}} = \{\alpha_{\mathrm{up,max}}^{\mathrm{s1}}, \alpha_{\mathrm{dn,max}}^{\mathrm{s1}}, c_{\mathrm{up,min}}^{\mathrm{R,s1}}, c_{\mathrm{up,max}}^{\mathrm{R,s1}}, c_{\mathrm{dn,min}}^{\mathrm{R,s1}}, c_{\mathrm{dn,max}}^{\mathrm{R,s1}}\} \tag{30}$$

$$\begin{cases} \alpha_{t,\mathrm{up}}^{\mathrm{s1}} = \dfrac{1}{P_t^{\mathrm{fl}}} \displaystyle\sum_{n=1}^{N_{\mathrm{T}}} (x_n^{\mathrm{up}} - P_{t,n}^{\mathrm{T,fl}}) \\ \alpha_{t,\mathrm{dn}}^{\mathrm{s1}} = \dfrac{1}{P_t^{\mathrm{fl}}} \displaystyle\sum_{n=1}^{N_{\mathrm{T}}} (P_{t,n}^{\mathrm{T,fl}} - x_n^{\mathrm{dn}}) \end{cases} \tag{31}$$

where x_n^{up} and x_n^{dn} are the temporary variables, and their function forms are shown in (32). The calculation method of penalty fees is shown in (33).

$$\begin{cases} \displaystyle\int_{P_{t,n}^{\mathrm{T,fl}}}^{x_n^{\mathrm{up}}} f_{\mathrm{up}}^{\mathrm{c1}}(P)\,\mathrm{d}P = 0 \quad \forall t,n \\ \displaystyle\int_{x_n^{\mathrm{dn}}}^{P_{t,n}^{\mathrm{T,fl}}} f_{\mathrm{dn}}^{\mathrm{c1}}(P)\,\mathrm{d}P = 0 \quad \forall t,n \end{cases} \tag{32}$$

$$\begin{cases} c_{t,\mathrm{up}}^{\mathrm{R,s1}} = \dfrac{\displaystyle\sum_{n=1}^{N_{\mathrm{T}}} (C_{t,\mathrm{up},n}^{\mathrm{fl,up}} + C_{t,\mathrm{dn},n}^{\mathrm{fl,up}} - C_{t,n}^{\mathrm{st,fl}} + C_{t,n}^{\mathrm{st,fl,up}})}{\Delta t \left[\Delta P_{t,\mathrm{up}}^{\mathrm{fl}} - \displaystyle\sum_{n=1}^{N_{\mathrm{T}}} (x_n^{\mathrm{up}} - P_{t,n}^{\mathrm{T,fl}}) \right]} \\ c_{t,\mathrm{dn}}^{\mathrm{R,s1}} = \dfrac{\displaystyle\sum_{n=1}^{N_{\mathrm{T}}} (C_{t,\mathrm{up},n}^{\mathrm{fl,dn}} + C_{t,\mathrm{dn},n}^{\mathrm{fl,dn}})}{\Delta t \left[\Delta P_{t,\mathrm{dn}}^{\mathrm{fl}} - \displaystyle\sum_{n=1}^{N_{\mathrm{T}}} (P_{t,n}^{\mathrm{T,fl}} - x_n^{\mathrm{dn}}) \right]} \end{cases} \tag{33}$$

After the grid sets the assessment indicators, RES can optimize the day-ahead power curve based on these indicators. Then, the grid calculates the power curve of thermal units based on the optimized power curve of RES, and the optimization objective still aims to minimize the RR cost. The calculation method of RR cost during each period is the same as (22)-(27), and will not be repeated here.

$$P_t^{\mathrm{L}} = P_t^{\mathrm{s1}} + \sum_{n=1}^{N_{\mathrm{T}}} P_{t,n}^{\mathrm{T,s1}} \quad \forall t \tag{34}$$

Here, an example is used to help explain the process of setting the assessment indicators in the day-ahead stage. Taking the positive direction as an example, the relationship between the usage and the cost of positive day-ahead RR during each period is shown in Fig. 5, and the positive day-ahead forecast deviation of RES is shown in Fig. 6(a). Assuming that $\alpha_{\mathrm{up,max}}^{\mathrm{s1}} = 0.1$ and $c_{\mathrm{up,min}}^{\mathrm{R,s1}} = 200$ ¥/MWh, the setting results of the day-ahead assessment indicators for the positive direction can be observed in Fig. 6.

As shown in Fig. 5, the cost of positive RR is relatively low around hours 0-6 and hours 11-12, and the total amount of RR provided for free can meet the demand of RES. Therefore, the deviation exemption ratio during these periods is set to be the base value $\alpha_{\mathrm{up,max}}^{\mathrm{s1}}$, and the penalty price is set to be the base value $c_{\mathrm{up,min}}^{\mathrm{R,s1}}$. However, the cost of positive RR is relatively high around hours 15-23, and even free RR cannot be provided. Therefore, the deviation exemption ratio $\alpha_{t,\mathrm{up}}^{\mathrm{s1}}$ is set to be 0, and the penalty price $c_{t,\mathrm{up}}^{\mathrm{R,s1}}$ is significantly higher than the base value during these periods. Positive RR in the grid is also abundant around hours 8-11, but the expected deviation power of RES is high during these periods,

as shown in Fig. 6, which means the RR demand is large. Therefore, although the assessment indicators during these periods are relatively loose, they are still stricter compared with hours 0-6 and hours 11-12. This example illustrates the main innovation of the proposed method for assessment indicators, which accurately conveys the grid reserve pressure to RES in real time considering RR supply capacity/price and expected deviation power of RES.

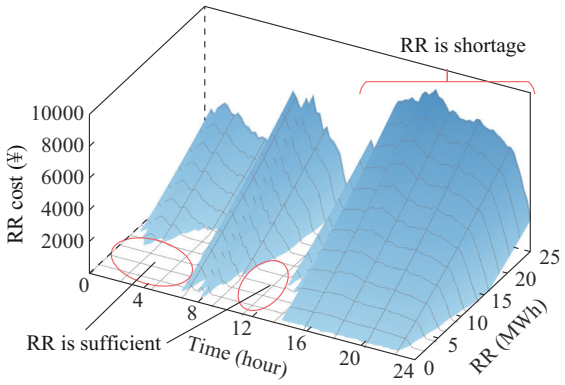

Fig. 5. Relationship between usage and cost of day-ahead positive RR during each period.

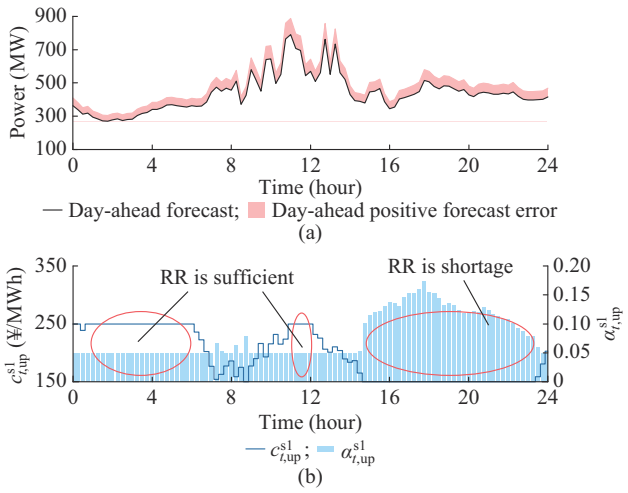

Fig. 6. Setting result of day-ahead positive assessment indicators. (a) Power. (b) $c^{s1}_{t,up}$ and $\alpha^{s1}_{t,up}$.

The above process initially calculates the values of assessment indicators. However, there is a certain deviation between the day-ahead power curve and the predicted power curve, which will change the load rate of thermal units and subsequently change the RR costs during each period. Therefore, the assessment indicators cannot accurately reflect the degree of RR scarity at this time. It is necessary to re-correct the assessment indicators using the day-ahead power curve declared by RES, and RES re-declares the power curve based on the corrected indicators. After several iterations, the rationality of the assessment indicators can be effectively improved.

2) Process of Setting Intraday Assessment Indicators

After entering the intraday stage, in addition to submitting the intraday power for period t to the grid at $t-2$, RES also needs to submit a rolling real-time forecast curve for the next 2 hours to the grid. The grid will then set intraday assessment indicators in real time based on the received RES forecast curve and the operating status of thermal units. RES will optimize the intraday power curve based on these indicators. According to the intraday power curve declared by RES, the grid will adjust the power curve of thermal units, and then settle the intraday RR cost and the intraday penalty cost that RES needs to pay.

The calculation process of RR fees during each intraday period is similar to that in the day-ahead stage, as shown in Appendix A. The difference is that when optimizing the power curve of each thermal unit, the RR cost $C^{s1}_{t,n}$ paid to adjust the day-ahead power curve of RES needs to be taken into account.

$$\min \sum_{n=1}^{N_T} (C^{f2}_{t,n}(D_{s2}) + C^{s1}_{t,n}(D_{s1})) \tag{35}$$

$$C^{s1}_{t,n} = C^{s1}_{t,up,n} + C^{s1}_{t,dn,n} \tag{36}$$

$$\begin{cases} C^{s1}_{t,up,n} = \Delta t \int_{P^{T,s1}_{t,n}}^{P^{T,f2}_{t,n}} f^{c1}_{up}(P)\,dP & \forall P^{T,f2}_{t,n} \geq P^{T,s1}_{t,n} \\ C^{s1}_{t,dn,n} = \Delta t \int_{P^{T,f2}_{t,n}}^{P^{T,s1}_{t,n}} f^{c1}_{dn}(P)\,dP & \forall P^{T,f2}_{t,n} < P^{T,s1}_{t,n} \end{cases} \tag{37}$$

Afterwards, the grid calculates the intraday power curves for each thermal unit based on the optimized intraday power curve provided by RES.

$$P^{L}_{t} = P^{s2}_{t} + \sum_{n=1}^{N_T} P^{T,s2}_{t,n} \quad \forall t \tag{38}$$

The base values are also necessary when setting the intraday assessment indicators. The methods for setting the intraday deviation exemption ratios ($\alpha^{s2}_{t,up}$, $\alpha^{s2}_{t,dn}$) and penalty prices ($c^{R,s2}_{t,up}$, $c^{R,s2}_{t,dn}$) are similar to the day-ahead stage. The difference between them is that the RR segmented prices of thermal units is replaced by $f^{c2}_{up}(\cdot)$ and $f^{c2}_{dn}(\cdot)$, and the probability density distribution function of the power forecast deviation ratio of RES is replaced by $f^{s2}_{t}(\cdot)$. For more details, please refer to Appendix A.

C. Evaluation of Assessment Indicator Setting Results

The rationality of the assessment indicator setting results can be evaluated from two aspects: ① whether the penalty fees paid by RES to the grid are sufficient to cover the RR costs paid by the grid to correct RES power deviations; ② whether RES can maintain a reasonable net income. The evaluation indicators are given in (39)-(43).

$$C^{R,s} = \sum_{t \in \Omega} C^{R,s}_{t} \tag{39}$$

$$C^{R,s}_{t} = C^{R,s1}_{t,up} + C^{R,s1}_{t,dn} + C^{R,s2}_{t,up} + C^{R,s2}_{t,dn} \tag{40}$$

$$C^{grid} = \sum_{t \in \Omega} (C^{s}_{t} - C^{R,s}_{t}) = C^{s} - C^{R,s} \tag{41}$$

$$C^{R}_{in} = \sum_{t \in \Omega} C^{R}_{t,in} \tag{42}$$

$$C^{R}_{t,in} = C^{R,e}_{t} - C^{BESS}_{t} - C^{R,s}_{t} \tag{43}$$

When C^{grid} is greater than 0, it means that the penalty fees paid by RES to the grid is sufficient to cover the RR costs, and when C^{grid} is less than 0, it means the RR assistance to RES will result in a loss. The optimization objective during

the setting of assessment indicators is given in (44), and the optimization needs to satisfy the constraint given in (45).

$$\max C_{\text{in}}^{\text{R}} \tag{44}$$

s.t.

$$C^{\text{grid}} \geq 0 \tag{45}$$

For the grid, a larger value of C^{grid} is preferable, but this part of the incomes may come from the assessment of RES. Blindly increasing the assessment standard for RES will harm the economic benefits of RES, which goes against the original intention of increasing the proportion of RES. Therefore, it is only necessary to keep C^{grid} within a range that the grid can afford, to maintain a balance between revenue and expenses. On this basis, the optimization objective is to maximize C_{in}^{R}.

III. Optimization Strategy for RES Power Curve

The BESS capacity self-equipped by RES is usually of small to medium scales, so the deviation correction ability of self-owned BESS is insufficient to completely correct the forecast deviation of RES. Therefore, although RES has power curve tracking ability, it still needs to adopt a certain power curve optimization strategy to effectively reduce power deviation.

A. Optimization Strategy of Day-ahead Power Curve

Before introducing the RES power curve optimization strategy, the modeling of the RES and the self-owned BESS should be established, which is given as:

$$0 \leq P_t^{\text{R}} \leq P_{\text{G}}^{\text{R}} \quad \forall t \tag{46}$$

$$-\delta_{\text{dn}}^{\text{R}} P_{\text{G}}^{\text{R}} \leq P_t^{\text{R}} - P_{t+1}^{\text{R}} \leq \delta_{\text{up}}^{\text{R}} P_{\text{G}}^{\text{R}} \quad \forall t \tag{47}$$

$$SOC_{t+1} = SOC_t + \frac{\Delta t}{Q_{\text{BESS}}}\left(\eta_{\text{ch}} P_t^{\text{ch}} - \frac{P_t^{\text{dch}}}{\eta_{\text{dch}}}\right) \tag{48}$$

$$\begin{cases} 0 \leq P_t^{\text{ch}} \leq \delta_{\text{ch}} Q_{\text{BESS}} / T_{\text{s}} \\ 0 \leq P_t^{\text{dch}} \leq \delta_{\text{dch}} Q_{\text{BESS}} / T_{\text{s}} \end{cases} \tag{49}$$

$$SOC_{\min} \leq SOC_t \leq SOC_{\max} \tag{50}$$

$$C_t^{\text{BESS}} = c_{\text{BESS}} Q_{\text{BESS}} \left| SOC_{t+1} - SOC_t \right| \tag{51}$$

When optimizing the day-ahead power curve of RES, the time scale between the optimization and actual generation is relatively long. Therefore, it is not suitable to predict the state of charge (SOC) curve of BESS. Due to the small capacity of the self-equipped BESS, if there is a forecast error, it will continuously affect the execution of the charging and discharging tasks for several subsequent periods, and the BESS will also be difficult to return to the expected operating trajectory. Therefore, in this paper, the expected deviation adjustment capacity P_{BESS} is used to reflect the role of BESS when optimizing the day-ahead power curve.

The optimization objective when calculating the day-ahead power curve is aimed to maximize $C_{t,\text{in}}^{\text{R,s1}}$:

$$\max C_{t,\text{in}}^{\text{R,s1}} \tag{52}$$

$$\begin{aligned} C_{t,\text{in}}^{\text{R,s1}} = \Delta t (& c_{\text{e}} P_t^{\text{s1}} - c_{t,\text{up}}^{\text{R,s1}} \Delta P_{t,\text{up}}^{\text{s1,f}} - c_{t,\text{dn}}^{\text{R,s1}} \Delta P_{t,\text{dn}}^{\text{s1,f}} - \\ & c_{\text{BESS}} P_{t,\text{up,s1}}^{\text{BESS}} - c_{\text{BESS}} P_{t,\text{dn,s1}}^{\text{BESS}}) \end{aligned} \tag{53}$$

$$P_t^{\text{R,f1}} = \int_0^{P_{t,\max}^{\text{s1}}} f^{\text{s1}}(r_t^{\text{f1}}) P \mathrm{d}P + \int_{P_{t,\max}^{\text{s1}}}^{P_{\text{G}}^{\text{R}}} f^{\text{s1}}(r_t^{\text{f1}}) P_{t,\max}^{\text{s1}} \mathrm{d}P \tag{54}$$

$$\begin{cases} \Delta P_{t,\text{up}}^{\text{s1,f}} = \displaystyle\int_{P_{t,\max}^{\text{s1}} + P_{t,\text{up,s1}}^{\text{BESS}}}^{P_{\text{G}}^{\text{R}}} (P - P_{t,\max}^{\text{s1}} - P_{t,\text{up,s1}}^{\text{BESS}}) f^{\text{s1}}(r_t^{\text{f1}}) \mathrm{d}P \\ \forall P_{\text{G}}^{\text{R}} \geq P_{t,\max}^{\text{s1}} + P_{t,\text{up,s1}}^{\text{BESS}} \end{cases} \tag{55}$$

$$\begin{cases} \Delta P_{t,\text{dn}}^{\text{s1,f}} = \displaystyle\int_0^{P_{t,\min}^{\text{s1}} - P_{t,\text{dn,s1}}^{\text{BESS}}} (P_{t,\min}^{\text{s1}} - P_{t,\text{dn,s1}}^{\text{BESS}} - P) f^{\text{s1}}(r_t^{\text{f1}}) \mathrm{d}P \\ \forall P_{t,\min}^{\text{s1}} - P_{t,\text{dn,s1}}^{\text{BESS}} \geq 0 \end{cases} \tag{56}$$

$$P_{t,\text{up,s1}}^{\text{BESS}} = \frac{1}{\eta_{\text{ch}} \eta_{\text{dch}}} P_{t,\text{dn,s1}}^{\text{BESS}} \quad \forall t \tag{57}$$

$$\begin{cases} 0 \leq P_{t,\text{up,s1}}^{\text{BESS}} \leq P_{\text{BESS}} \quad \forall t \\ 0 \leq P_{t,\text{dn,s1}}^{\text{BESS}} \leq P_{\text{BESS}} \quad \forall t \end{cases} \tag{58}$$

$$P_{\text{BESS}} = 0.5 N_{\text{day}} (SOC_{\max} - SOC_{\min}) Q_{\text{BESS}} \eta_{\text{ch}} \eta_{\text{dch}} / \Delta t \tag{59}$$

where P_{BESS} is a decision variable that affects the optimization results.

If the positive and negative forecast errors of the RES do not have a significant difference in the long-term operation, the average SOC of the BESS should be around 0.5. Therefore, according to the range of SOC, the capacity of BESS, and the charging and discharging efficiencies of BESS, P_{BESS} can be calculated. Since the capacity of the self-equipped BESS is small, the ability of returning the SOC to the reference point ($SOC = 0.5$) must be considered in the long-term operation, that is, the charging and discharging amount must maintain dynamic balance. Therefore, $P_{t,\text{up,s1}}^{\text{BESS}}$ and $P_{t,\text{up,s2}}^{\text{BESS}}$ for each period should be kept equal after considering the charging and discharging efficiencies.

B. Optimization Strategy of Intraday Power Curve

When optimizing the intraday power curve, the forecast accuracy of RES is significantly improved compared with that of day-ahead power curve, and their actual generation time is relatively close. At this time, the predicted SOC curve can be used to improve the ability of BESS to correct power deviations.

According to the day-ahead power curve, intraday forecast curve, and current SOC, the charging and discharging power can be estimated for the time interval $[t-2, t-0.25]$.

$$\begin{cases} P_t^{\text{ch,f}} = \Delta P_{t,\text{up}}^{\text{tag}} - \Delta P_{t,\text{dn}}^{\text{tag}} & \forall \Delta P_{t,\text{up}}^{\text{tag}} \geq \Delta P_{t,\text{dn}}^{\text{tag}} \\ P_t^{\text{dch,f}} = \Delta P_{t,\text{dn}}^{\text{tag}} - \Delta P_{t,\text{up}}^{\text{tag}} & \forall \Delta P_{t,\text{up}}^{\text{tag}} < \Delta P_{t,\text{dn}}^{\text{tag}} \end{cases} \tag{60}$$

$$r_t^{\text{f2}} = (P - P_t^{\text{f2}}) / P_t^{\text{f2}} \tag{61}$$

$$\begin{cases} \Delta P_{t,\text{up}}^{\text{tag}} = \displaystyle\int_{P_{t,\max}^{\text{s2}}}^{P_{\text{G}}^{\text{R}}} f^{\text{s2}}(r_t^{\text{f2}})(P - P_{t,\max}^{\text{s2}}) \mathrm{d}P \\ \Delta P_{t,\text{dn}}^{\text{tag}} = \displaystyle\int_0^{P_{t,\min}^{\text{s2}}} f^{\text{s2}}(r_t^{\text{f2}})(P_{t,\min}^{\text{s2}} - P) \mathrm{d}P \end{cases} \tag{62}$$

This example is used to demonstrate the process of predicting the SOC trajectory, as shown in Fig. 7. The expected charging and discharging power of BESS in the time interval $[t-2, t-0.25]$ (a total of 7 scheduling periods and each period is 15 min) is shown in Fig. 7(a), and the initial SOC of BESS is 0.5, $Q_{\text{BESS}} = 100$ MWh, $SOC_{\max} = 0.9$, $SOC_{\min} = 0.1$, $\eta_{\text{ch}} = \eta_{\text{dch}} = 0.95$, and $\delta_{\text{ch}} = \delta_{\text{dch}} = 2$. The predicted SOC curve

during different periods is shown in Fig. 7(b).

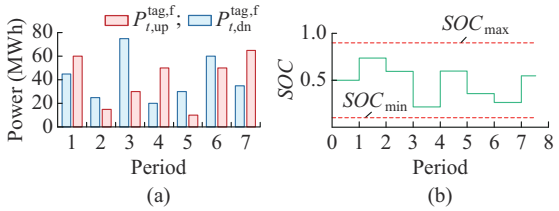

Fig. 7. Relationship between use of day-ahead positive RR and RR cost during each period. (a) Expected charging and discharging power of BESS. (b) Predicted SOC curve.

The process shown in Fig. 7 can be used to predict the SOC of the BESS during the target period and then calculate the expected intraday deviation adjustment ability of the BESS during that period. After that, the power curve can be optimized based on intraday forecast deviations and day-ahead deviations. The method for calculating intraday forecast deviations is similar to day-ahead stage, as described in Appendix A. The objective to optimize the intraday power curve of RES is shown in (63)-(65).

$$\max C_{t,\mathrm{in}}^{\mathrm{R,s2}} \tag{63}$$

$$C_{t,\mathrm{in}}^{\mathrm{R,s2}} = \Delta t(c_{\mathrm{e}} P_t^{\mathrm{s2}} - c_{t,\mathrm{up}}^{\mathrm{R,s1}} \Delta P_{t,\mathrm{up}}^{\mathrm{s1}} - c_{t,\mathrm{dn}}^{\mathrm{R,s1}} \Delta P_{t,\mathrm{dn}}^{\mathrm{s1}} - c_{t,\mathrm{up}}^{\mathrm{R,s2}} \Delta P_{t,\mathrm{up}}^{\mathrm{s2,f}} - c_{t,\mathrm{dn}}^{\mathrm{R,s2}} \Delta P_{t,\mathrm{dn}}^{\mathrm{s2,f}} - c_{\mathrm{BESS}} P_{t,\mathrm{up,s2}}^{\mathrm{BESS}} - c_{\mathrm{BESS}} P_{t,\mathrm{dn,s2}}^{\mathrm{BESS}}) \tag{64}$$

$$\begin{cases} P_{t,\mathrm{up,s2}}^{\mathrm{BESS}} = (SOC_{\max} - SOC_{t-1}^{\mathrm{f}}) Q_{\mathrm{BESS}} \eta_{\mathrm{ch}} \\ P_{t,\mathrm{dn,s2}}^{\mathrm{BESS}} = (SOC_{t-1}^{\mathrm{f}} - SOC_{\min}) Q_{\mathrm{BESS}} / \eta_{\mathrm{dch}} \end{cases} \tag{65}$$

When RES starts actual generation, the strategy for using BESS is to correct the intraday deviation as much as possible by combining real-time power forecast, intraday power curve, and the remaining control capacity of BESS.

IV. Case Study

This section mainly addresses three issues: ① the impact of the value range on the rationality of the assessment indicators setting results; ② the advantages of dynamic setting of assessment indicators compared with using fixed assessment indicators; ③ the impact of the RES power curve optimization strategy designed in this paper on the income of RES.

A. Scene Data

The parameters of G1-G3 and RES in the grid are shown in Tables II and III, respectively, and the segmented RR prices of G1-G3 are shown in Table I. The probability density functions of the day-ahead and intraday forecast error ratios of RES, i.e., $f^{\mathrm{s1}}(\cdot)$ and $f^{\mathrm{s2}}(\cdot)$, are shown in Fig. 8(a) and 8(b), respectively. The parameters of the BESS owned by RES are set as: $Q_{\mathrm{BESS}} = 100$ MWh, $SOC_{\max} = 0.9$, $SOC_{\min} = 0.1$, $\eta_{\mathrm{ch}} = \eta_{\mathrm{ch}} = 0.95$, $\delta_{\mathrm{ch}} = \delta_{\mathrm{dch}} = 2$, and $c_{\mathrm{BESS}} = 700$ ¥/MWh. The electricity price in power grid is $c_{\mathrm{e}} = 400$ ¥/MWh. The setting iteration of assessment indicators is $m_{\max} = 3$. The simulation runs for 30 days. The day-ahead forecast curve of RES and load curve are shown in Fig. 9.

B. Impact of Range of Assessment Indicators

The range of assessment indicators will significantly affect the effectiveness of the setting method.

TABLE II
Parameters of Units

Unit	$P_{\mathrm{G}}^{\mathrm{T}}$ (MW)	$\delta_{\mathrm{up}}^{\mathrm{T}}$	$\delta_{\mathrm{dn}}^{\mathrm{T}}$	$P_{\max}^{\mathrm{T}}$ (MW)	$P_{\min}^{\mathrm{T}}$ (MW)
G1	500	0.3	0.3	500	150
G2	300	0.3	0.3	300	90
G3	200	0.3	0.3	200	60

TABLE III
Parameters of RES

$P_{\mathrm{G}}^{\mathrm{R}}$ (MW)	$\delta_{\mathrm{up}}^{\mathrm{R}}$	$\delta_{\mathrm{dn}}^{\mathrm{R}}$	$P_{\max}^{\mathrm{R}}$ (MW)	$P_{\min}^{\mathrm{R}}$ (MW)
500	1.5	1.5	500	0

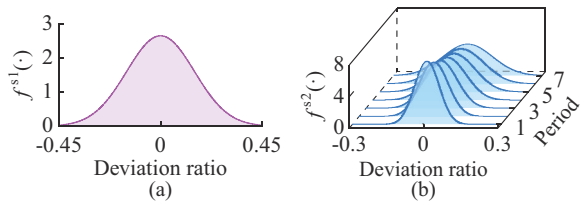

Fig. 8. Probability density function of forecast deviation. (a) $f^{\mathrm{s1}}(\cdot)$. (b) $f^{\mathrm{s2}}(\cdot)$.

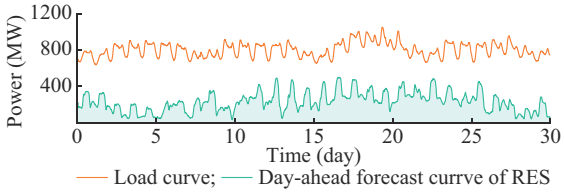

Fig. 9. Day-ahead forecast curve of RES and load curve.

First, based on the RR pricing table of thermal units, the base value of penalty price can be calculated. Assuming that the RR in the region is very scarce and the units always operate in the highest RR price, $c_{\mathrm{up,max}}^{\mathrm{R,s1}}$ and $c_{\mathrm{dn,max}}^{\mathrm{R,s1}}$ can be set as 800 ¥/MWh, and $c_{\mathrm{up,max}}^{\mathrm{R,s2}}$ and $c_{\mathrm{dn,max}}^{\mathrm{R,s2}}$ can be set as 1200 ¥/MWh. In actual operation, RR is not always in a state of scarcity, so setting the above upper limits for penalty fees is reasonable.

Based on this, the range of assessment indicators in different scenarios is shown in Table IV. The RR cost C^{s}, penalty cost $C^{\mathrm{R,s}}$, and profit of RES $C_{\mathrm{in}}^{\mathrm{R}}$ in Cases 1-16 are calculated when the scenarios shown in Section III-A are used, as shown in Fig. 10 and Table V.

When there is sufficient RR in the grid, the values of the deviation exemption ratios may be high, and the penalty price may be zero because the free RR can cover the expected deviation of RES. In the dynamic setting process, this situation will be restricted. The base values of deviation exemption ratios and penalty prices represent the minimum assessment standards that RES must accept. If the base values of deviation exemption ratios are low and/or the base values of the penalty prices are high, it can be considered that RES accepts stricter assessments on average. Cases 1-16 increase the strictness of RES assessment by reducing the base values of deviation exemption ratios or/and increasing the base value of the penalty prices. The penalty fee C^{s} shows an increasing trend, with the penalty fees in Case 16, being the

most stringent assessment, increasing by ¥3.8536×10^6 compared with the most lenient assessment in Case 1.

TABLE IV
RANGE OF ASSESSMENT INDICATORS

Case	$\alpha^{s1}_{up,max}$ and $\alpha^{s1}_{dn,max}$	$c^{R,s1}_{up,min}$ and $c^{R,s1}_{dn,min}$ (¥/MWh)	$\alpha^{s2}_{up,max}$ and $\alpha^{s2}_{dn,max}$	$c^{R,s2}_{up,min}$ and $c^{R,s2}_{dn,min}$ (¥/MWh)
1		0		0
2	0.20	0	0.100	0
3	0.10	0	0.050	0
4	0.05	0	0.025	0
5	0.20	100	0.100	200
6	0.10	100	0.050	200
7	0.05	100	0.025	200
8	0.20	150	0.100	300
9	0.10	150	0.050	300
10	0.05	150	0.025	300
11	0.20	200	0.100	400
12	0.10	200	0.050	400
13	0.05	200	0.025	400
14	0.20	300	0.100	500
15	0.10	300	0.050	500
16	0.05	300	0.025	500

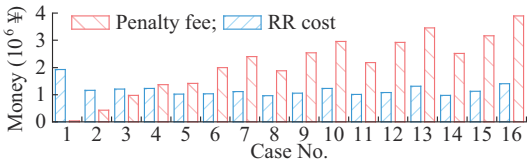

Fig. 10. Penalty fee and RR cost in different cases.

TABLE V
C^{grid} AND C^R_{in} IN DIFFERENT CASES

Case No.	C^{grid} (10^6 ¥)	C^R_{in} (10^6 ¥)	$C^{grid}+C^R_{in}$ (10^6 ¥)
1	–1.8913	66.5147	64.6234
2	–0.7194	66.3985	65.6791
3	–0.2338	65.5061	65.2723
4	0.1299	64.9343	65.0642
5	0.3953	65.0633	65.4586
6	0.9598	64.6100	65.5698
7	1.2809	63.8325	65.1134
8	0.9186	64.8559	65.7745
9	1.4834	63.6218	65.1052
10	1.7257	63.2813	65.0070
11	1.1725	63.8652	65.0377
12	1.8381	63.3947	65.2328
13	2.1419	62.5798	64.7217
14	1.5478	63.1712	64.7190
15	2.0441	62.9867	65.0308
16	2.4912	62.7189	65.2101

Meanwhile, the profit of RES C^R_{in} decreases from ¥66.5147×10^6 to ¥62.7189×10^6 due to the increase in assessment standard. However, the RR cost does not decrease monotonically as assessment strictness increases, such as the RR cost of ¥0.4431×10^6 in Case 16 being higher than the lowest RR cost in Case 8. The reason is as follows. If RES accepts overly strict assessment standards when the RR is sufficient, it may result in conservative optimization of the power curve. At this time, the operating trajectory of the thermal units may deviate significantly from their original plan. The RR scarcity/price is related to the load rate of thermal power units. Changing the power curve may reduce the RR that thermal units can provide or increase the price, which can make the setting results of original assessment indicator no longer reasonable. As a result, RES may accept strict assessment standards, but it could cause RR to become even scarcer. Similarly, if the assessment indicators have no base values, such as in Case 1, the power curve optimization result of RES may be too aggressive, causing a significant deviation of the load rate of thermal power units from the expected trajectory.

In summary, setting value ranges for assessment indicators is intended to reduce the impact of changes in the power curves of the thermal power units on the degree of RR scarity.

In Case 8, the revenue and expenditure of the grid tend to balance, and C^{grid} is ¥0.9186×10^6, so it can be considered that the constraint of formula (45) is satisfied, and the profit of RES is relatively large, i.e., C^R_{in} is ¥65.7745×10^6. At this time, the interests of both the grid and RES are guaranteed. If the grid and RES are viewed as a whole, the value of their joint benefit $C^{grid}+C^R_{in}$ is also relatively large in Case 8. Therefore, the assessment range in Case 8 is the optimal choice.

C. Advantages of Dynamically Tuning Indicators

This subsection focuses on discussing the advantages of dynamic assessment indicators compared with fixed assessment indicators. When using Case 8, the average values of each assessment indicator are shown in (66)-(69).

$$\begin{cases}\alpha^{s1}_{t,up,max}=0.070640\\ \alpha^{s1}_{t,dn,max}=0.162545\end{cases} \tag{66}$$

$$\begin{cases}c^{R,s1}_{t,up,min}=399.708\\ c^{R,s1}_{t,dn,min}=198.939\end{cases} \tag{67}$$

$$\begin{cases}\alpha^{s2}_{t,up,max}=0.040169\\ \alpha^{s2}_{t,dn,max}=0.084096\end{cases} \tag{68}$$

$$\begin{cases}c^{R,s2}_{t,up,min}=583.658\\ c^{R,s2}_{t,dn,min}=349.229\end{cases} \tag{69}$$

Assuming the fixed assessment indicators use the average values shown in (66)-(69) during each period, the RR costs of the grid and the profit of RES are calculated, and the results are compared with dynamic assessment indicators in this paper, as shown in Table VI.

TABLE VI
COMPARISON OF IMPLEMENTATION EFFECT WHEN USING FIXED AND DYNAMIC ASSESSMENT INDICATORS

Parameter	C^s (10^6 ¥)	$C^{R,s}$ (10^6 ¥)	C^{grid} (10^6 ¥)	C^R_{in} (10^6 ¥)	$C^{grid}+C^R_{in}$ (10^6 ¥)
Fixed	4.1922	2.4623	–1.7299	63.8968	62.1669
Dynamic	0.9572	1.8758	0.9186	64.8559	65.7745

When using fixed assessment indicators, the values of C^{s} and $C^{R,s}$ are both higher compared with using dynamic assessment indicators. It means that RES is under higher plan tracking pressure without alleviating the RR scarcity of the grid, leading to a 5.8031% decrease in the comprehensive benefit $C^{grid}+C^{R}_{in}$. This situation is mainly caused by the difference in the time distribution of RR supply capacity. Taking Fig. 11 as an example, the time distribution of the day-ahead positive assessment indicators $\alpha^{s1}_{t,up}$ and $c^{R,s1}_{t,up}$ for positive RR can be observed. The periods with sufficient RR ($\alpha^{s1}_{t,up}=0.2$, $c^{R,s1}_{t,up}=0$) and those with scarce RR ($\alpha^{s1}_{t,up}=0$) both account for a considerable proportion. This indicates that the adjustment capability of thermal power units varies significantly at different time. In the scenario shown in this example, a considerable proportion of the periods do not experience RR scarcity, so only some periods need to implement strict plan assessment. Other periods can use standard assessment indicators to reduce power curve tracking pressure of RES. On average, the assessment indicators are not overly strict, but this does not mean that the requirement for power curve tracking capability of RES is reduced. Rather, the valuable adjustment capacity is utilized more during the periods when RR is scarce.

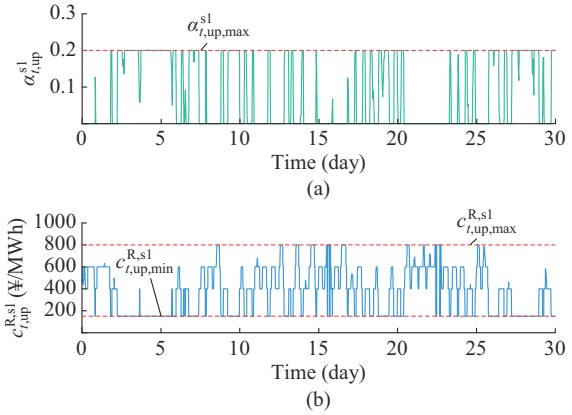

Fig. 11. Dynamic setting results of positive day-ahead assessment indicators. (a) $\alpha^{s1}_{t,up}$. (b) $c^{R,s1}_{t,up}$.

D. Impact of RES Power Curve Optimization Strategy and Self-owned BESS Capacity

In this paper, the management mode of RES shifts from a forecast error management mode to a power curve assessment mode. At this point, RES cannot only declare the original forecast curve; it needs to optimize the power curve based on the adjustment of its self-owned BESS capability and assessment indicators. Under the same set of assessment indicators, optimizing the power curve reasonably can effectively increase the profit of RES. This subsection will compare the profits of RES using the proposed power curve optimization strategy and directly declaring the power forecast curve.

As shown in Table VII, when directly reporting the forecast power curve, the penalty fee $C^{R,s}$ increases significantly, with an increase of ¥6.0355×10^{6} compared with using the proposed power curve optimization strategy, and the net profit of RES decreases by 11.5052%. This indicates it can effectively avoid penalty risks by optimizing the power curve and improve the net profit of RES. In addition, when directly reporting the original power forecast curve, C^{R}_{in} decreases by ¥6.6919×10^{6}, and the decrease in C^{R}_{in} is greater than the increase in penalty fees. This suggests that the proposed power curve optimization strategy does not reduce the grid-connected electricity of RES due to increasing plan tracking capability, but at the same time, increasing the profit of RES. Therefore, the reasonable optimization of the power curve is not simple to lower the forecast curve, but to dynamically adjust the strategy based on the strictness of the assessment. RES can appropriately raise the curve during the periods with looser assessment to increase the grid-connected electricity.

TABLE VII
COMPARISON OF IMPLEMENTATION EFFECTS BETWEEN DIRECTLY DECLARING FORECAST POWER CURVE AND USING OPTIMIZED POWER CURVE

Strategy	C^{s} (10^{6} ¥)	$C^{R,s}$ (10^{6} ¥)	C^{grid} (10^{6} ¥)	C^{R}_{in} (10^{6} ¥)	$C^{grid}+C^{R}_{in}$ (10^{6} ¥)
Without strategy	5.7669	7.9113	2.1444	58.1640	60.3084
With proposed strategy	0.9572	1.8758	0.9186	64.8559	65.7745

The capacity of the self-owned BESS is a key parameter affecting the deviation correction capability of RES. Assuming Q_{BESS} ranges from 0 to 200 MWh, the penalty fees are calculated using the assessment indicators shown in Case 8, and the results are shown in Fig. 12.

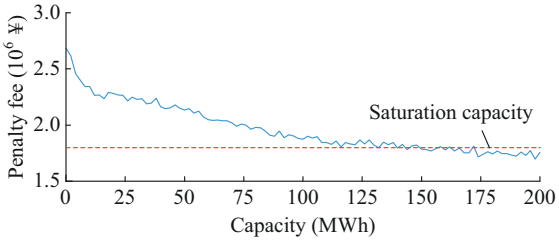

Fig. 12. Penalty fees with different BESS capacities.

The penalty fee without equipping BESS for RES is ¥2.6865×10^{6}, which is increased by 30.1768% compared with that equipping 100 MWh of BESS. This indicates that the self-owned BESS can effectively reduce power deviation. However, equipping BESS with excessively high capacity cannot continue to reduce the penalty fees. When equipping 200 MWh of BESS, the penalty fee is ¥1.7560×10^{6}, with little improvement compared with that equipping 100 MWh of BESS. The reason is that some power deviations can be corrected by modifying the power curve and paying a certain penalty cost. If a large amount of valuable BESS is used to correct the day-ahead power deviation, the correction ability of the intraday power deviation will decrease, which is equivalent to giving up high-value targets. Therefore, in this paper, BESS is more focused on correcting intraday power deviation. RES needs to reasonably plan the capacity of its self-owned BESS, ensuring both deviation correction capabilities and avoiding redundant equipping.

V. Conclusions

This paper proposes a dynamic setting method for assessment indicators that considers the RR scarcity and a power curve optimization strategy for RES that considers self-owned BESS.

1) This paper dynamically sets the assessment indicators based on the distribution of RR supply capacity and prices at different time. In this way, the degree of RR scarcity can be accurately conveyed to RES in real time, which helps maintain the supply and demand balance of RR. Compared with using fixed indicators, this method is conducive to reducing RR costs and increasing RES profits.

2) When setting the indicators, a certain range of values should be set, and the assessment indicators should not be relaxed without limit to avoid misleading RES. By optimizing the range of assessment indicator values, the rationality of the setting results can be improved.

3) Reasonable analysis of the deviation adjustment ability of BESS combined with forecast errors when optimizing the power curve can effectively reduce penalty costs and increase RES profits. The optimized power curve can also help the grid reduce RR costs.

4) The capacity of the self-owned BESS is a key parameter affecting the deviation adjustment ability of RES. However, BESS is not the only way to adjust deviations, and some deviations are more suitable for correction by adjusting the power curve. Therefore, there is a saturation capacity for self-owned BESS.

Appendix A

The supplemental formulas for the intraday assessment indicators setting process are given as:

$$\begin{cases} \Delta P_{t,\mathrm{up}}^{\mathrm{f2}} = \displaystyle\int_{P_t^{\mathrm{f2}}}^{P_{\mathrm{G}}^{\mathrm{R}}} f^{\mathrm{s2}}(r_t^{\mathrm{f2}})(P - P_t^{\mathrm{f2}})\mathrm{d}P \\ \Delta P_{t,\mathrm{dn}}^{\mathrm{f2}} = \displaystyle\int_{0}^{P_t^{\mathrm{f2}}} f^{\mathrm{s2}}(r_t^{\mathrm{f2}})(P_t^{\mathrm{f2}} - P)\mathrm{d}P \end{cases} \tag{A1}$$

$$r_t^{\mathrm{f2}} = (P - P_t^{\mathrm{f2}})/P_t^{\mathrm{f2}} \tag{A2}$$

$$P_t^{\mathrm{L}} = P_t^{\mathrm{f2}} + \sum_{n=1}^{N_{\mathrm{T}}} P_{t,n}^{\mathrm{T,f2}} \quad \forall t \tag{A3}$$

$$P_t^{\mathrm{L}} = P_t^{\mathrm{f2}} + \Delta P_{t,\mathrm{up}}^{\mathrm{f2}} + \sum_{n=1}^{N_{\mathrm{T}}} P_{t,n}^{\mathrm{T,f2,up}} \quad \forall t \tag{A4}$$

$$P_t^{\mathrm{L}} = P_t^{\mathrm{f2}} - \Delta P_{t,\mathrm{dn}}^{\mathrm{f2}} + \sum_{n=1}^{N_{\mathrm{T}}} P_{t,n}^{\mathrm{T,f2,dn}} \quad \forall t \tag{A5}$$

$$\begin{cases} C_{t,\mathrm{up},n}^{\mathrm{f2,up}} = \Delta t \displaystyle\int_{P_{t,n}^{\mathrm{T,f2}}}^{P_{t,n}^{\mathrm{T,f2,up}}} f_{\mathrm{up}}^{\mathrm{c2}}(P)\,\mathrm{d}P \quad \forall P_{t,n}^{\mathrm{T,f2,up}} \geq P_{t,n}^{\mathrm{T,f2}} \\ C_{t,\mathrm{dn},n}^{\mathrm{f2,up}} = \Delta t \displaystyle\int_{P_{t,n}^{\mathrm{T,f2,up}}}^{P_{t,n}^{\mathrm{T,f2}}} f_{\mathrm{dn}}^{\mathrm{c2}}(P)\,\mathrm{d}P \quad \forall P_{t,n}^{\mathrm{T,f2,up}} < P_{t,n}^{\mathrm{T,f2}} \end{cases} \tag{A6}$$

$$\begin{cases} C_{t,\mathrm{up},n}^{\mathrm{f2,dn}} = \Delta t \displaystyle\int_{P_{t,n}^{\mathrm{T,f2}}}^{P_{t,n}^{\mathrm{T,f2,dn}}} f_{\mathrm{up}}^{\mathrm{c2}}(P)\,\mathrm{d}P \quad \forall P_{t,n}^{\mathrm{T,f2,dn}} \geq P_{t,n}^{\mathrm{T,f2}} \\ C_{t,\mathrm{dn},n}^{\mathrm{f2,dn}} = \Delta t \displaystyle\int_{P_{t,n}^{\mathrm{T,f2,dn}}}^{P_{t,n}^{\mathrm{T,f2}}} f_{\mathrm{dn}}^{\mathrm{c2}}(P)\,\mathrm{d}P \quad \forall P_{t,n}^{\mathrm{T,f2,dn}} < P_{t,n}^{\mathrm{T,f2}} \end{cases} \tag{A7}$$

$$\begin{cases} C_{t,n}^{\mathrm{st,f2}} = c_{\mathrm{st}} P_{\mathrm{G},n}^{\mathrm{T}} \Delta u_{t,n}^{\mathrm{f2}} \\ C_{t,n}^{\mathrm{st,f2,up}} = c_{\mathrm{st}} P_{\mathrm{G},n}^{\mathrm{T}} \Delta u_{t,n}^{\mathrm{f2,up}} \\ C_{t,n}^{\mathrm{st,f2,dn}} = c_{\mathrm{st}} P_{\mathrm{G},n}^{\mathrm{T}} \Delta u_{t,n}^{\mathrm{f2,dn}} \end{cases} \tag{A8}$$

$$D_{\mathrm{s2}} = \{\alpha_{\mathrm{up,max}}^{\mathrm{s2}}, \alpha_{\mathrm{dn,max}}^{\mathrm{s2}}, c_{\mathrm{up,min}}^{\mathrm{R,s2}}, c_{\mathrm{up,max}}^{\mathrm{R,s2}}, c_{\mathrm{dn,min}}^{\mathrm{R,s2}}, c_{\mathrm{dn,max}}^{\mathrm{R,s2}}\} \tag{A9}$$

$$\begin{cases} \alpha_{t,\mathrm{up}}^{\mathrm{s2}} = \dfrac{1}{P_t^{\mathrm{f2}}} \displaystyle\sum_{n=1}^{N_{\mathrm{T}}} (x_n^{\mathrm{up}} - P_{t,n}^{\mathrm{T,f2}}) \\ \alpha_{t,\mathrm{dn}}^{\mathrm{s2}} = \dfrac{1}{P_t^{\mathrm{f2}}} \displaystyle\sum_{n=1}^{N_{\mathrm{T}}} (P_{t,n}^{\mathrm{T,f2}} - x_n^{\mathrm{dn}}) \end{cases} \tag{A10}$$

where x_n^{up} and x_n^{dn} are temporary variables, and their function forms are shown in (A11).

$$\begin{cases} \displaystyle\int_{P_{t,n}^{\mathrm{T,f2}}}^{x_n^{\mathrm{up}}} f_{\mathrm{up}}^{\mathrm{c2}}(P)\,\mathrm{d}P = 0 \quad \forall t,n \\ \displaystyle\int_{x_n^{\mathrm{dn}}}^{P_{t,n}^{\mathrm{T,f2}}} f_{\mathrm{dn}}^{\mathrm{c2}}(P)\,\mathrm{d}P = 0 \quad \forall t,n \end{cases} \tag{A11}$$

$$\begin{cases} c_{t,\mathrm{up}}^{\mathrm{R,s2}} = \dfrac{\displaystyle\sum_{n=1}^{N_{\mathrm{T}}} (C_{t,\mathrm{up},n}^{\mathrm{f2,up}} + C_{t,\mathrm{dn},n}^{\mathrm{f2,up}} - C_{t,n}^{\mathrm{st,f2}} + C_{t,n}^{\mathrm{st,f2,up}})}{\Delta t \left[\Delta P_{t,\mathrm{up}}^{\mathrm{f2}} - \displaystyle\sum_{n=1}^{N_{\mathrm{T}}} (x_n^{\mathrm{up}} - P_{t,n}^{\mathrm{T,f2}}) \right]} \\ c_{t,\mathrm{dn}}^{\mathrm{R,s2}} = \dfrac{\displaystyle\sum_{n=1}^{N_{\mathrm{T}}} (C_{t,\mathrm{up},n}^{\mathrm{f2,dn}} + C_{t,\mathrm{dn},n}^{\mathrm{f2,dn}})}{\Delta t \left[\Delta P_{t,\mathrm{dn}}^{\mathrm{f2}} - \displaystyle\sum_{n=1}^{N_{\mathrm{T}}} (P_{t,n}^{\mathrm{T,f2}} - x_n^{\mathrm{dn}}) \right]} \end{cases} \tag{A12}$$

$$\begin{cases} \alpha_{t,\mathrm{up}}^{\mathrm{s2}} \in [0, \alpha_{\mathrm{up,max}}^{\mathrm{s2}}] \quad \forall t \\ \alpha_{t,\mathrm{dn}}^{\mathrm{s2}} \in [0, \alpha_{\mathrm{dn,max}}^{\mathrm{s2}}] \quad \forall t \end{cases} \tag{A13}$$

$$\begin{cases} c_{t,\mathrm{up}}^{\mathrm{R,s2}} \in [c_{\mathrm{up,min}}^{\mathrm{R,s2}}, c_{\mathrm{up,max}}^{\mathrm{R,s2}}] \quad \forall t \\ c_{t,\mathrm{dn}}^{\mathrm{R,s2}} \in [c_{\mathrm{dn,min}}^{\mathrm{R,s2}}, c_{\mathrm{dn,max}}^{\mathrm{R,s2}}] \quad \forall t \end{cases} \tag{A14}$$

The supplementary formulas for the intraday power curve optimization strategy are given as:

$$P_t^{\mathrm{R,f2}} = \int_0^{P_{t,\max}^{\mathrm{s2}}} f^{\mathrm{s2}}(r_t^{\mathrm{f2}}) P \mathrm{d}P + \int_{P_{t,\max}^{\mathrm{s2}}}^{P_{\mathrm{G}}^{\mathrm{R}}} f^{\mathrm{s2}}(r_t^{\mathrm{f2}}) P_{t,\max}^{\mathrm{s2}} \mathrm{d}P \tag{A15}$$

$$\begin{cases} \Delta P_{t,\mathrm{up}}^{\mathrm{s2,f}} = \displaystyle\int_{P_{t,\max}^{\mathrm{s2}} + P_{t,\mathrm{up,s2}}^{\mathrm{BESS}}}^{P_{\mathrm{G}}^{\mathrm{R}}} (P - P_{t,\max}^{\mathrm{s2}} - P_{t,\mathrm{up,s2}}^{\mathrm{BESS}}) f^{\mathrm{s2}}(r_t^{\mathrm{f2}}) \mathrm{d}P \\ P_{\mathrm{G}}^{\mathrm{R}} \geq P_{t,\max}^{\mathrm{s2}} + P_{t,\mathrm{up,s2}}^{\mathrm{BESS}} \end{cases} \tag{A16}$$

$$\begin{cases} \Delta P_{t,\mathrm{dn}}^{\mathrm{s2,f}} = \displaystyle\int_{0}^{P_{t,\min}^{\mathrm{s2}} - P_{t,\mathrm{dn,s2}}^{\mathrm{BESS}}} (P_{t,\min}^{\mathrm{s2}} - P_{t,\mathrm{dn,s2}}^{\mathrm{BESS}} - P) f^{\mathrm{s2}}(r_t^{\mathrm{f2}}) \mathrm{d}P \\ P_{t,\min}^{\mathrm{s2}} - P_{t,\mathrm{dn,s2}}^{\mathrm{BESS}} \geq 0 \end{cases} \tag{A17}$$

References

[1] X. Zhou, Q. Zhao, Y. Zhang *et al.*, "Integrated energy production unit: An innovative concept and design for energy transition toward low-carbon development," *CSEE Journal of Power and Energy Systems*, vol. 7, no. 6, pp. 1133-1139, Nov. 2021.

[2] W. Zhou, Q. Chen, D. Luo *et al.*, "Global energy consumption analysis based on the three-dimensional network model," *IEEE Access*, vol. 8, pp. 76313-76332, Apr. 2020.

[3] Y. Jiang, X. Chen, K. Yu *et al.*, "Short-term wind power forecasting using hybrid method based on enhanced boosting algorithm," *Journal of Modern Power Systems and Clean Energy*, vol. 5, no. 1, pp. 126-133, Jan. 2017.

[4] A. Bharatee, P. K. Ray, and A. Ghosh, "A power management scheme for grid-connected PV integrated with hybrid energy storage system," *Journal of Modern Power Systems and Clean Energy*, vol. 10, no. 4, pp. 954-963, Jul. 2022.
[5] F. Gu, S. Lu, J. Wu *et al*., "Interruptible power estimation and auxiliary service allocation using contract theory and dynamic game for demand response in aggregator business model," *IEEE Access*, vol. 7, pp. 129975-129987, Sept. 2019.
[6] Z. Tan, K. Chen, L. Ju *et al*., "Issues and solutions of China's generation resource utilization based on sustainable development," *Journal of Modern Power Systems and Clean Energy*, vol. 4, no. 2, pp. 147-160, Apr. 2016.
[7] Z. Zhang, M. Zhou, Z. Wu *et al*., "A frequency security constrained scheduling approach considering wind farm providing frequency support and reserve," *IEEE Transactions on Sustainable Energy*, vol. 13, no. 2, pp. 1086-1100, Apr. 2022.
[8] E. A. Bakirtzis and P. N. Biskas, "Multiple time resolution stochastic scheduling for systems with high renewable penetration," *IEEE Transactions on Power Systems*, vol. 32, no. 2, pp. 1030-1040, Mar. 2017.
[9] L. Zhang, K. Meng, Y. Jia *et al*., "A multistep wind speed forecasting system considering double time series features," *IEEE Access*, vol. 8, pp. 161018-161030, Sept. 2020.
[10] B. Mohandes, M. Wahbah, M. S. E. Moursi *et al*., "Renewable energy management system: optimum design and hourly dispatch," *IEEE Transactions on Sustainable Energy*, vol. 12, no. 3, pp. 1615-1628, Jul. 2021.
[11] Y. Gong, C. Y. Chung, and R. S. Mall, "Power system operational adequacy evaluation with wind power ramp limits," *IEEE Transactions on Power Systems*, vol. 33, no. 3, pp. 2706-2716, May 2018.
[12] J. Zheng, Y. Kou, M. Li *et al*., "Stochastic optimization of cost-risk for integrated energy system considering wind and solar power correlated," *Journal of Modern Power Systems and Clean Energy*, vol. 7, no. 6, pp. 1472-1483, Nov. 2019.
[13] M. Hedayati-Mehdiabadi, J. Zhang, and K. W. Hedman, "Wind power dispatch margin for flexible energy and reserve scheduling with increased wind generation," *IEEE Transactions on Sustainable Energy*, vol. 6, no. 4, pp. 1543-1552, Oct. 2015.
[14] D. A. Halamay, T. K. A. Brekken, A. Simmons *et al*., "Reserve requirement impacts of large-scale integration of wind, solar, and ocean wave power generation," *IEEE Transactions on Sustainable Energy*, vol. 2, no. 3, pp. 321-328, Jul. 2011.
[15] W. Wang, S. Huang, G. Zhang *et al*., "Optimal operation of an integrated electricity-heat energy system considering flexible resources dispatch for renewable integration," *Journal of Modern Power Systems and Clean Energy*, vol. 9, no. 4, pp. 699-710, Jul. 2021.
[16] Y. Fang, S. Zhao, E. Du *et al*., "Coordinated operation of concentrating solar power schedulet and wind farm for frequency regulation," *Journal of Modern Power Systems and Clean Energy*, vol. 9, no. 4, pp. 751-759, Jul. 2021.
[17] E. Ela, V. Gevorgian, A. Tuohy *et al*., "Market designs for the primary frequency response ancillary service – Part I: motivation and design," *IEEE Transactions on Power Systems*, vol. 29, no. 1, pp. 421-431, Jan. 2014.
[18] E. Ela, V. Gevorgian, A. Tuohy *et al*., "Market designs for the primary frequency response ancillary service – Part II: case studies," *IEEE Transactions on Power Systems*, vol. 29, no. 1, pp. 432-440, Jan. 2014.
[19] D. H. Blum, T. Zakula, and L. K. Norford, "Opportunity cost quantification for ancillary services provided by heating, ventilating, and air-conditioning systems," *IEEE Transactions on Smart Grid*, vol. 8, no. 3, pp. 1264-1273, May 2017.
[20] O. Alkadi, N. Cappers, P. Denholm *et al*., "Demand response for ancillary services," *IEEE Transactions on Smart Grid*, vol. 4, no. 4, pp. 1988-1995, Dec. 2013.
[21] T. K. Chau, S. Yu, T. Fernando *et al*., "Demand-side regulation provision from industrial loads integrated with solar PV panels and energy storage system for ancillary services," *IEEE Transactions on Industrial Informatics*, vol. 14, no. 11, pp. 5038-5049, Nov. 2018.
[22] M. Bahloul and S. K. Khadem, "Impact of power sharing method on battery life extension in HESS for grid ancillary services," *IEEE Transactions on Energy Conversion*, vol. 34, no. 3, pp. 1317-1327, Sept. 2019.
[23] Y. Yoo, S. Jung, and G. Jang, "Dynamic inertia response support by energy storage system with renewable energy integration substation," *Journal of Modern Power Systems and Clean Energy*, vol. 8, no. 2, pp. 260-266, Mar. 2020.
[24] S. Ganesan, U. Subramaniam, A. A. Ghodke *et al*., "Investigation on sizing of voltage source for a battery energy storage system in microgrid with renewable energy sources," *IEEE Access*, vol. 8, pp. 188861-188874, Oct. 2020.
[25] S. B. Elghali, R. Outbib, and M. Benbouzid, "Selecting and optimal sizing of hybridized energy storage systems for tidal energy integration into power grid," *Journal of Modern Power Systems and Clean Energy*, vol. 7, no. 1, pp. 113-122, Jan. 2019.
[26] F. R. Albogamy, M. Y. I. Paracha, G. Hafeez *et al*., "Real-time scheduling for optimal energy optimization in smart grid integrated with renewable energy sources," *IEEE Access*, vol. 10, pp. 35498-35520, Mar. 2022.
[27] J. Martinez-Rico, E. Zulueta, I. R. de Argandoña *et al*., "Multi-objective optimization of production scheduling using particle swarm optimization algorithm for hybrid renewable power schedulets with battery energy storage system," *Journal of Modern Power Systems and Clean Energy*, vol. 9, no. 2, pp. 285-294, Mar. 2021.
[28] T. Li and M. Dong, "Real-time residential-side joint energy storage management and load scheduling with renewable integration," *IEEE Transactions on Smart Grid*, vol. 9, no. 1, pp. 283-298, Jan. 2018.

Minghao Cao received the B.S. degree from Zhengzhou University, Zhengzhou, China, in 2018, and the M.S. degree from Harbin Institute of Technology, Harbin, China, in 2020. He is working toward the Ph.D in electrical engineering in Harbin Institute of Technology. His research interests include renewable energy dispatch and grid planning.

Jilai Yu received the B.S. and Ph.D. degrees from Harbin Institute of Technology, Harbin, China, in 1992. He joined the Department of Electrical Engineering, Harbin Institute of Technology, in 1992, where he is currently a Professor of the Electric Power Research Institute. His current research interests include power system analysis and control, optimal dispatch of power system, green power, and smart grid.